

Deep learning assessment of syllable affiliation of intervocalic consonants

Zirui Liu,^{1,a} Yi Xu^{1, b}

¹ *Speech, Hearing and Phonetic Sciences, University College London, London, WC1N 1PJ, United Kingdom*

In English, a sentence like “He made out our intentions.” could be misperceived as “He may doubt our intentions.” because the coda /d/ sounds like it has become the onset of the next syllable. The nature and the occurrence condition of this resyllabification phenomenon are unclear, however. Previous empirical studies mainly relied on listener judgment, limited acoustic evidence such as voice onset time (VOT) or average formant values to determine the occurrence of resyllabification. This study tested the hypothesis that resyllabification is a coarticulatory re-organisation that realigns the coda consonant with the vowel of the next syllable. We used deep learning in conjunction with dynamic time warping (DTW) to assess syllable affiliation of intervocalic consonants. The results suggest that convolutional and recurrent neural network (CNN-RNN) based models can detect cases of resyllabification using Mel-frequency spectrograms. DTW analysis shows that neural network inferred resyllabified sequences are acoustically more similar to their onset counterparts than their canonical productions. A binary classifier further

^azirui.liu.17@ucl.ac.uk

^byi.xu@ucl.ac.uk

24 suggests that similar to the genuine onsets, the inferred resyllabified coda
25 consonants are coarticulated with the following vowel. These results are
26 interpreted with an account of resyllabification as a speech-rate-dependent
27 coarticulatory reorganisation mechanism in speech.

28 I. INTRODUCTION

29 Despite the wide recognition of the syllable as a speech unit among
30 speakers and researchers (Browman & Goldstein, 1992; Levelt, Roelofs &
31 Meyer, 1999; MacNeilage, 1998), there have been doubts about the role of
32 the syllable due to ambiguity associated with syllable boundaries. One
33 situation where ambiguity is especially severe is in regard to the syllable
34 affiliation of intervocalic consonants. For example, the phrase “escort us” in
35 British English (/ɛs#k:ɔt#əs/) can be syllabified as /ɛs#k:ɔ#təs / in
36 connected speech, according to observation of a noisy release during the
37 word final /t/ (Levelt et al., 1999). The phenomenon is more formally known
38 as resyllabification, which usually denotes a shift of syllabification of a coda
39 consonant into the onset of the following vowel-initial syllable (Levelt et al.,
40 1999; Schiller et al., 1997). For English, empirical work examining
41 resyllabification goes back as early as 70 years ago, when Stetson used the
42 kymograph to investigate CV and VC production at different speech rates
43 (Stetson, 1951). He observed that in a sequence of syllables like /bi bi bi.../,
44 the CV structure remains stable regardless of speech rate. In contrast, a
45 sequence of VC syllables such as /ib ib ib.../, becomes very similar to /bi bi
46 bi.../ when repeated at a fast rate, according to kymograph data, indicating
47 that the coda /b/ is resyllabified as an onset consonant. The perceptual
48 finding was consistent with articulatory patterns recorded by the
49 kymograph. Stetson’s findings were later replicated by Tuller and Kelso
50 (1990, 1991), with glottal transillumination data, which showed that glottal

51 movements shifted drastically at a critical rate of speech, and perception of
52 the spoken sequences also shifted to be mostly identified as /ip ip ip.../.

53 In languages such as Spanish and French (Bermúdez-Otero, 2011, Gaskell
54 et al., 2002), resyllabification is recognised as a phonological process,
55 although there are cross dialect variations according to acoustic evidence
56 such as consonantal duration (Strycharczuk & Kohlberger, 2016). Due to
57 the lack of clear empirical evidence, the existence of resyllabification in
58 English is questioned (Shattuck-Hufnagel, 2011), as mentioned above.

59 Furthermore, the status of the syllable is called into question because of
60 boundary ambiguity due to resyllabification (Blevins, 2003; Steriade, 1999).

61 A major source of the difficulty of determining the syllabification status of
62 segments is that it is mainly based on the subjective judgment of listeners
63 (Ní Chiosáin et al., 2012; Content, 2001; Goslin & Frauenfelder, 2001;
64 Schiller et al., 1997). Even when acoustic measurements are taken, listener
65 judgments are still treated as the “ground truth” (de Jong et al., 2004;
66 Mullooly, 2003). But as found in de Jong et al. (2004), listeners agree with
67 each other well only in cases where a gap between the release of the coda
68 consonant and the beginning of voicing for the next vowel can be easily
69 detected. In the absence of apparent gaps, listener judgments become very
70 diverse. Those authors therefore suggested that the difference between the
71 coda and onset consonant is more closely related to how they are
72 *motorically optimised* in production in ways that are too subtle for most
73 listeners to detect.

74 What is needed is an alternative definition of resyllabification, that departs
75 from conventional definitions that are based on language-specific
76 phonotactics (what is phonologically legal), perceptual impression, and
77 language-specific acoustic properties (aspiration, voicing, etc.). In this
78 study, we consider an articulatory-acoustic definition that specifies the
79 affiliation of an intervocalic consonant based on an articulatory definition of
80 the syllable. And the definition of the syllable, as will be reviewed next, also
81 addresses coarticulation, another essential issue of speech articulation.

82 **A. Resyllabification, coarticulation and the syllable**

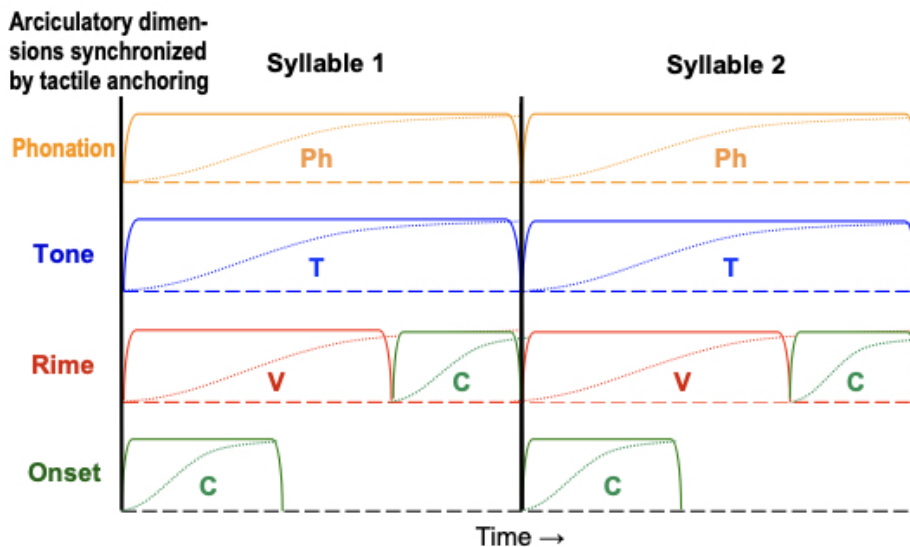
83 Resyllabification is closely related to a well-documented asymmetry
84 between onset and coda consonants in both phonology and phonetics. For
85 languages that allow for coda consonants, codas are more vulnerable than
86 their onset counterparts, as they are more susceptible to deletion and
87 reduction (Barlow & Gierut, 1999; Xu, 1986, 2020). In contrast, onset
88 consonants are often inserted when the syllable is vowel initial, such as
89 glottal stop insertion (Birgit, 2001; Garellek, 2012), intrusive /r/s (Gick,
90 1999; Uffmann, 2007), and vowel hiatus breakers (Mudzingwa, 2013; Smith,
91 2001). In terms of canonical syllable structures, CV syllables are also more
92 common than both VC and CVC syllables in many languages (Clements &
93 Keyser, 1983; Levelt et al., 1999; Xu, 2020).

94 According to articulatory phonology, the vulnerability of codas is likely
95 related to an asymmetry in coarticulation within the syllable. That is, onset

96 consonants are coupled “in-phase” with the vowel, resulting in synchronous
97 activation between the vocalic and onset C gestures (Goldstein et al., 2006).
98 On the other hand, coda consonants are coupled “anti-phase” with the
99 vowel, which is a less stable mode of coordination. Resyllabification is
100 therefore “analysed as an abrupt transition to a more stable coordination
101 mode” that is likely to occur under increased speaking rate (Goldstein et al.,
102 2006:237).

103 An alternative account of resyllabification is provided by the
104 synchronisation model of the syllable (Xu, 2020), as shown in Fig. 1, which
105 shares some similarities with articulatory phonology but differs from it in
106 certain critical details. The model assumes that syllable is a mechanism for
107 eliminating most of the temporal degrees of freedom by synchronising
108 consonant, vowel and glottal movements at syllable onset (vertical lines),
109 whereby each movement (dotted lines) is to approach an underlying target
110 within its allocated time interval. The synchronisation makes the initial
111 consonant fully overlapped, hence coarticulated, with the initial portion of
112 the “following” vowel. In contrast, a coda consonant is articulated
113 sequentially after the vowel, because its closing movement directly conflicts
114 with the opening movement of the vowel (Xu & Liu, 2006). There are two
115 differences between this model and articulatory phonology that are directly
116 relevant for the current study. First, synchronisation is assumed to be a
117 fundamental design of the syllable (likely centrally controlled) rather than
118 emerging from the coupling of the gestural planning oscillators as in

119 articulatory phonology (Goldstein et al., 2006). Second, the sequential
 120 articulation of coda consonant is not modelled in terms of phase relation
 121 between C and V, because a) individual target approximation movements
 122 are frequently allocated insufficient amount of times (Nakatani et al., 1981;
 123 Xu & Wang, 2009), thus disallowing them to form complete movement
 124 cycles (Xu & Prom-on, 2019), and b) syllables constantly vary their duration,
 125 due to stress, phrasing and other linguistic factor, which makes it difficult
 126 for syllable sequences, together with their constituent segments, to be
 127 temporally periodic to make oscillation-based modelling possible.

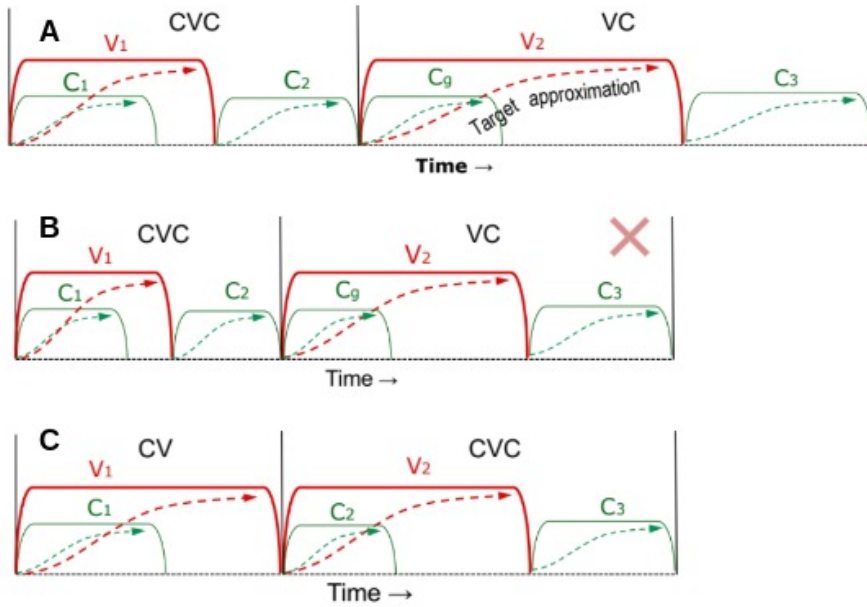


128

129 FIG. 1. The synchronisation model of the syllable (Xu, 2020).

130 According to the synchronisation model of the syllable, resyllabification is
 131 due to a lack of articulation time, as schematised in Fig. 2, rather than due
 132 to transition from anti-phase to in-phase articulatory coordination. In Fig.
 133 2A, the coda consonant (C_2) occupies its own time interval because it is

134 sequentially articulated after the first vowel (V_1). Meanwhile, the second
135 syllable is not articulated as a true VC because it actually starts with a
136 glottal stop (C_g). Such glottal stops have been reported as frequently
137 occurring at slow speech rate (Birgit, 2001; de Jong, 2001), but would
138 disappear as speech rate reached a certain threshold, leading to a
139 perceptual shift from /VC#VC/ to /CV#CV/ (de Jong, 2001). As illustrated in
140 Fig. 2B, as speech rate increases, less time is allocated to the syllable,
141 which would require the duration for both V_1 and C_2 to be shortened to an
142 implausible extent (as indicated by the red cross). The increased time
143 pressure (Tiffany, 1980; Xu & Prom-on, 2019) may then lead to the
144 replacement of the glottal stop (C_g) with C_2 when speech rate approaches a
145 certain threshold (e.g. 350 ms per syllable (de Jong, 2001)). C_2 now
146 becomes the initial consonant of the second syllable, as shown in Fig. 2C.
147 This reorganisation gives V_1 more articulation time while preserving all the
148 segmental composition of the original syllables.



149

150 FIG. 2. Illustration of articulatory resyllabification based on the
151 synchronisation model of the syllable.

152 Based on this account of resyllabification, two predictions can be made: 1)
153 Due to similarity in articulatory structure, resyllabified codas spectrally
154 resemble their onset counterparts more than their canonical form, and the
155 opposite can be observed for the non NN-resyllabified ones. 2) Because a
156 resyllabified coda is fully coarticulated with the vowel of the following
157 syllable, there is similar amount of vowel information shared between the
158 resyllabified onsets and the canonical onsets, but not between canonical
159 codas and canonical onsets. These predictions can be tested on English by
160 applying machine learning models on acoustic data.

B. Using deep neural networks with acoustic data to identify resyllabification

Given the difficulty of subjectively judging the occurrence of resyllabification (de Jong et al., 2004), an alternative is to obtain objective evidence by taking advantages of recent development in machine learning technology. This study therefore aims to determine the occurrences of resyllabification using deep learning models and dynamic time warping in combination with continuous acoustic data. The deep learning models used were inspired by state-of-the-art automatic speech recognition (ASR) networks (Amodei et al., 2015). ASR systems without language models are error prone when detecting the canonical structure of resyllabified sequences (Adda-Decker et al., 2002; Mirzaei et al., 2018; Wu et al., 1997). For example, a sequence like “fade out” could be recognised as “Fay doubt” if the coda /d/ is resyllabified as the onset of the second syllable. We trained recognition networks on slow speech data with no resyllabification occurrences and used them to classify data from normal rate speech. The reason behind using data from the slow speech rate condition for training is to ensure that there are no resyllabified sequences in the training data. In other words, for the model to be able to misclassify a sequence as its onset counterpart due to resyllabification, it should not be trained with a resyllabified sequence labelled as its canonical version. The misclassified sequences in normal speech rate (i.e. “fade out” as “fay doubt”) were further examined to shed some light on the articulatory structure of the syllable.

184 **II. Methods**

185 We trained a deep neural network classifier to identify word sequences such
186 as “coo part” and “coop art”. The utterances in the slow condition were
187 used for training the classifiers. Then, we used the trained classifiers to
188 classify the same utterances spoken in the normal rate recordings. A
189 /CVC#VC/ sequence such as ‘coop art’ was categorised as resyllabified if
190 the classifier “misclassified” it as its counterpart /CV#CVC/ sequence, i.e.
191 ‘coo part’. These neural network inferred resyllabified sequences are
192 referred to as NN-resyllabified to avoid confusion between the cognitive
193 process of syllable reorganisation and the inferred syllabification status by
194 the classifier. Dynamic time warping was then used to investigate the
195 spectral similarities between the NN-resyllabified sequences in the normal
196 speaking rate and the sequences in the slow rate (e.g. NN-resyllabified
197 “coop art” vs. slow “coo part” or NN-resyllabified “coop art” vs. non
198 resyllabified slow “coop art”). Furthermore, to test prediction (2), we built
199 binary neural network classifiers to categorise contrastive pairs such as
200 “coop art” vs. “coop eat”, whose training data only consisted of the
201 intervocalic consonantal portions of the acoustic signal (e.g. aspiration
202 for /p/). The closure interval was not included due to very little acoustic
203 energy in the data, as /p/ is a voiceless stop. The results were compared
204 between speech rates and syllable structures.

A. Subjects

Eight subjects aged 20-40 participated in this study, whose first language was Southern Standard British English (6 female and 2 males). No speaking or hearing disorders were reported prior to recording. To ensure data quality, all potential participants had to submit a short recording on Gorilla. The experimenters then visually inspected the recordings in the computer program Praat (Boersma & Weenink, 2022). Only participants with an external microphone and sufficient recording quality took part in the study.

B. Stimuli and data collection

Table I lists the word sequences used in this study. The stimuli include three groups of four sequences. For each group, the onset pair and coda pair match in terms of segments and differ in syllable structure, e.g. /CVC#VC/ vs. /CV#CVC/. This maximises the possibility that if the classifier misclassified a coda sequence as its onset counterpart, it is likely due to the shift in syllable structure, i.e. resyllabification.

TABLE I. Stimuli.

Group	Onset		Coda	
1	Lee steal	Lee stale	Least eel	Least ale
2	Do mart	Do meet	Doom art	Doom eat
3	Coo part	Coo Pete	Coop art	Coop eat

221 Note that there exist differences other than syllabification between onset
222 and coda sequences, such as lexical, syntactic or prosodic properties. For
223 example, “doom art” is a noun/verb noun sequence, where as “do mart” is a
224 verb noun sequence. The neural network classifier could use information
225 such as syllabification, syntactic and lexical differences between the onset
226 and coda tokens. Therefore, it is important to minimise the *similarities*
227 between items such as “coo part” and “coop art” due to the following: If the
228 classifier misclassified “coop art” as “coo part”, it is important to minimise
229 the possibility that the misclassification took place due to prosodic or lexical
230 similarity between the two, rather than coarticulation between the
231 intervocalic C and the second V. Therefore, within each onset and coda pair,
232 we use word combinations that differ in their morphosyntactic structure
233 (e.g. “Lee steal” vs. “least eel”). However, other unknown factors may still
234 result in similarities between the onset and coda pairs which could
235 contribute to misclassification. The current design can only assume that
236 when a coda sequence is misclassified as its onset counterpart, it is due to
237 similarity in coarticulation structure rather than other unknown factors.

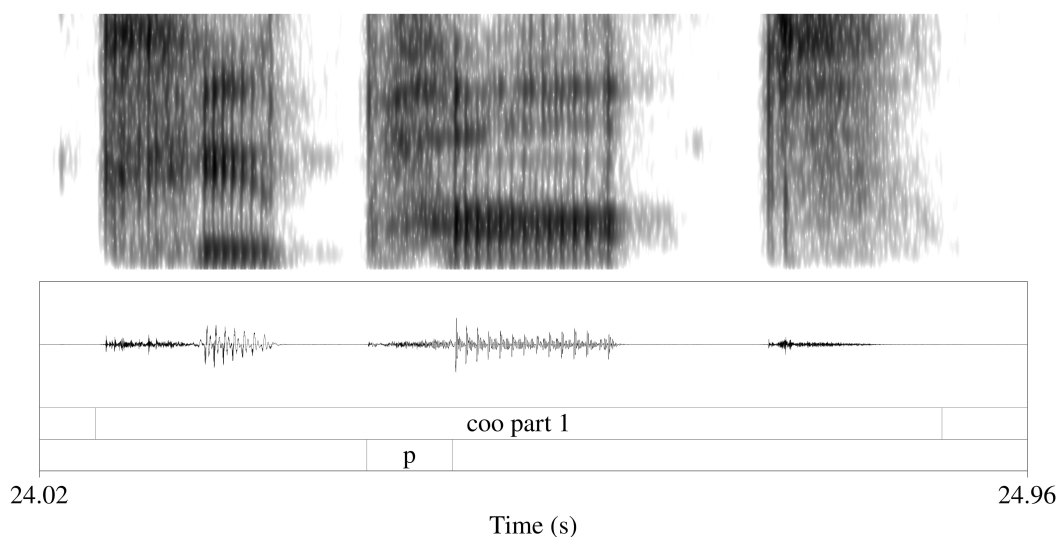
238 There is also a vowel minimal contrast in the second syllable for each
239 syllable structure condition in each group. The vowel contrast allows us to
240 examine the amount of coarticulation in the intervening consonant, by
241 assessing the performance of a binary classifier at predicting the second
242 vowel identity using only acoustic data from the annotated consonant
243 interval. Previous studies have used a minimal pair design and showed that

244 when a consonant is coarticulated with the upcoming vowel, acoustic
245 information associated with the vowel can be detected during the consonant
246 (Liu & Xu, 2021, Liu et al., 2022). Liu and Xu (2021) also show that the
247 entire cluster in /clusterV/ syllables in British English is coarticulated with
248 the vowel. Thus, a cluster triplet is included in the current study to
249 investigate whether the following vowel is coarticulated from the onset of
250 the consonant cluster.

251 Participants were instructed to say the word sequences in isolation in two
252 blocks of different speaking rates – first slow, then normal. For the slow
253 block, the speakers were instructed to articulate the words clearly and
254 fluently, at a slow pace. In the normal condition, speakers were informed to
255 speak at a faster pace in a colloquial style. There were no instructions on
256 what resyllabification was, or whether they should or should not resyllabify
257 anything. The stimuli were read aloud with 20 and 10 repetitions for the
258 randomised slow and normal blocks, respectively, yielding 360 tokens per
259 speaker ($12 \times 20 + 12 \times 10$). Around 3% of the data were excluded due to
260 background noise during recording.

261 The recording took place online over Zoom with the sampling rate of 32
262 kHz, with Zoom's original sound feature turned on, which preserved the
263 original recording quality by minimising the amount of audio enhancement.
264 All the participants used an external microphone during the experiment and
265 the recording quality was assessed by the researcher prior to the

266 experiment. For the resyllabification classifiers, the recordings were
 267 annotated in either $[C_1V_1\#C_2V_2C_2]$ or $[C_1V_1C_1\#V_2C_2]$ format (subscripts
 268 denote syllable position), with the first boundary being the start of acoustic
 269 landmark of onset C_1 (e.g. lateral murmur for /l/), and the second boundary
 270 being the end of acoustic landmark of the coda C_2 . For the binary classifiers,
 271 the consonantal intervals were segmented as the plosive aspiration for /p/,
 272 nasal murmur for /m/ and frication for /s/. An example is shown in Fig. 3.

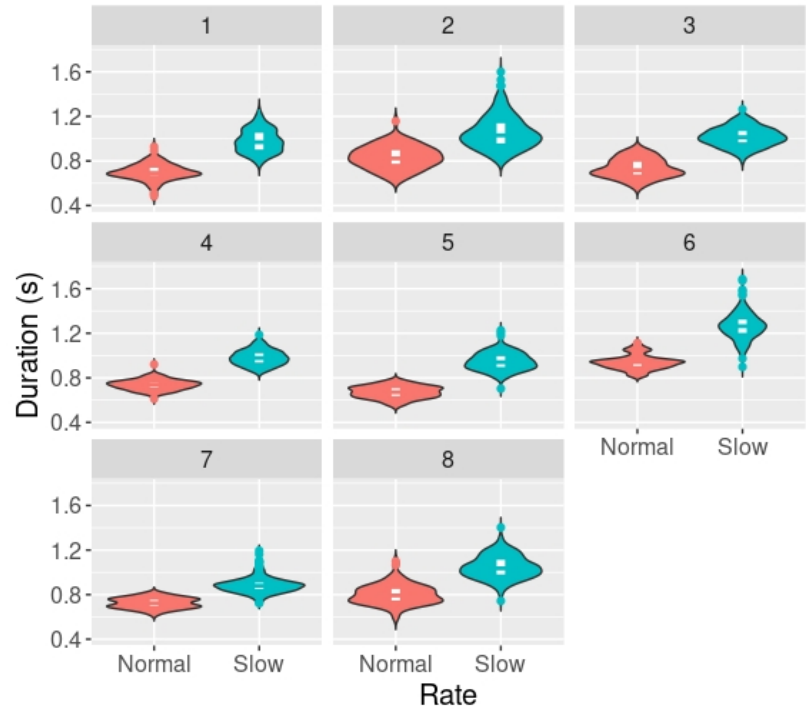


273
 274 FIG. 3. An annotation example of “coo part” from one speaker, with the
 275 vertical lines indicating the segmentations.

276 C. Speech rate analysis

277 As speech tempo can be speaker-specific due to difference in speaker
 278 characteristic (Jacewicz et al., 2009), participants were free to speak at a
 279 rate they deemed appropriate as slow or normal. For both the slow and

280 normal rate condition, participants were instructed to speak fluently (i.e.
281 without spontaneous pausing). No spontaneous pauses were identified in
282 the data during the annotation process. Therefore, speech rate in the
283 present study is analogous to articulation rate, which does not include
284 hesitation, pausing or emotional expressions. The duration values of
285 annotated tokens are presented in Fig. 4. As the figure shows, speech rate
286 was faster for the normal condition compared to the slow condition for all
287 speakers. On average, speakers produced 2.9 syllables per second for the
288 normal rate and 2 syllables per second for the slow rate. According to de
289 Jong (2001), resyllabification should take place when articulation rate
290 approaches 2.8 syllables per second.



291
292 FIG. 4. Annotated sequence duration for 8 speakers.

D. Neural network classifier for identifying resyllabification

1. Data preparation

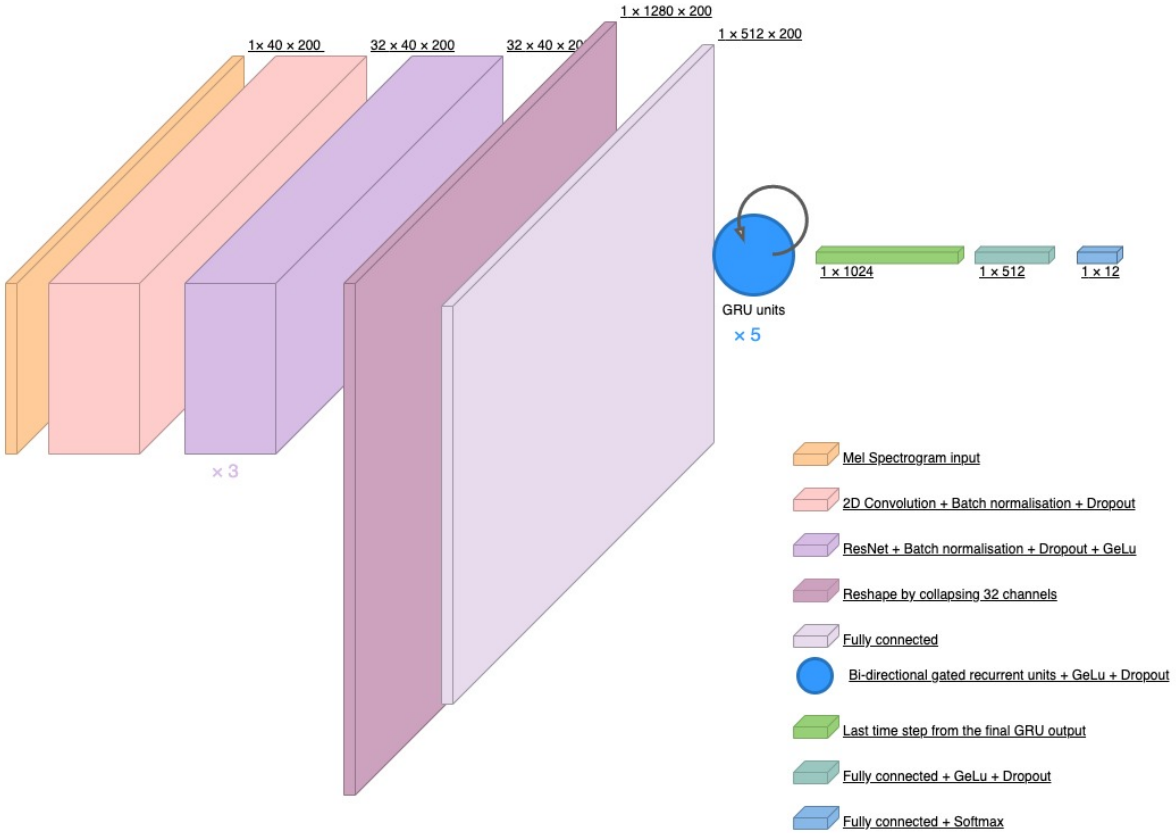
To ensure high accuracy, neural networks were trained for each speaker individually. The segmented word sequences from the slow condition were converted into mel-frequency spectrograms with 40 mel filter-banks with 25 ms as the window length and a hopping interval of 5 ms. We augmented the data to boost the amount of training data by using common augmentation techniques, such as speed augmentation, noise addition and frequency/time masking (Ko et al., 2015; Park et al., 2019). First, half of the tokens from the speaker were selected and sped up randomly between the factor of 0.3 to 0.9, by using the Audacity software with a custom Python script (Audacity Team, 2021). This resulted in 360 samples per speaker. Then, 15% of the resultant dataset were reserved as the testing set ($N = 54$), and 85% as the training set ($N = 306$)¹. Note that the samples were randomised before data splitting. Since the original data are balanced between word classes, the train and test split should also contain approximately balanced data, resultant of the random sampling process. The training set was then further boosted by augmenting 30% with random Gaussian noise addition to the raw acoustic signal (Pervaiz et al., 2020), or frequency or time masking to the spectrograms (Park et al., 2019), yielding 398 samples for the training set. Not only does data augmentation improve model generalisation and performance, the sped-up samples also familiarise the model with shorter acoustic signal such as those in the normal speech rate condition. The

motivation for doing noise addition and masking boost after the speed boost is to provide the benefit of these augmentation techniques for the sped-up tokens as well rather than just the original slow sequences.

2. Model architecture

The model architecture is shown in Fig. 5², which was inspired by a combination of Deep Speech and ResNet, developed by Baidu (Amodei et al., 2015) and Microsoft (He et al., 2015), respectively. Each model was trained for 120 epochs, unless the average accuracy across the last 5 epochs has reached the threshold of 98% for the testing set. For each epoch, the spectrograms were padded to the same duration as the longest sequence in the batch ($N = 32$), then fed into the neural network. Note that Fig. 5 demonstrates the flow of data through the network by a batch size of 1. The spectrogram is first passed through a 2D convolutional layer (i.e. convolutional neural network (CNN)), which had a 3×3 kernel with a stride of 1, and 32 channels. The output from the 2D convolutional layer is then passed through 3 residual blocks (He et al., 2015), the convolutional layers in each residual block had a 5×5 kernel with a stride of 1. For both the 2D convolutional and residual layers, padding was used to retain the shape of the tensors. The motivation behind these two types of convolutional layers is for the model to extract features such as dynamic information of spectral energy between frequencies or time steps (e.g. velocity of energy variation between time steps) (Luo et al., 2018; Sharma et al., 2020). To preserve as much acoustic information as possible, no

pooling was used. The output from the residual layers was reshaped by collapsing the 32 channels, resulting in tensors with the shape of 1280 by n timesteps, which was further reduced by a fully connected layer with 512 units. Five layers of bi-directional Gated Recurrent Units (GRU) were then used to process the sequential acoustic features. Only the last timestep's output was used from the GRU. Finally, the output was fed into two fully connected layers with a final SoftMax activation which generated the 12-dimensional probability vector, one for each word sequence in Table I. Due to the complexity of the model, we used dropout as the regularisation technique to combat overfitting (Semeniuta et al., 2016). A dropout rate of 0.1 was used throughout the network (see Fig. 5 for dropout locations). Furthermore, batch normalisation was applied after each mini batch to stabilise learning, as well as provide some regularisation effect (Ioffe & Szegedy, 2015). The hyperparameters were tuned by using grid search with data from the pilot study. The hyperparameters used can be found in Table II in the Appendix section.



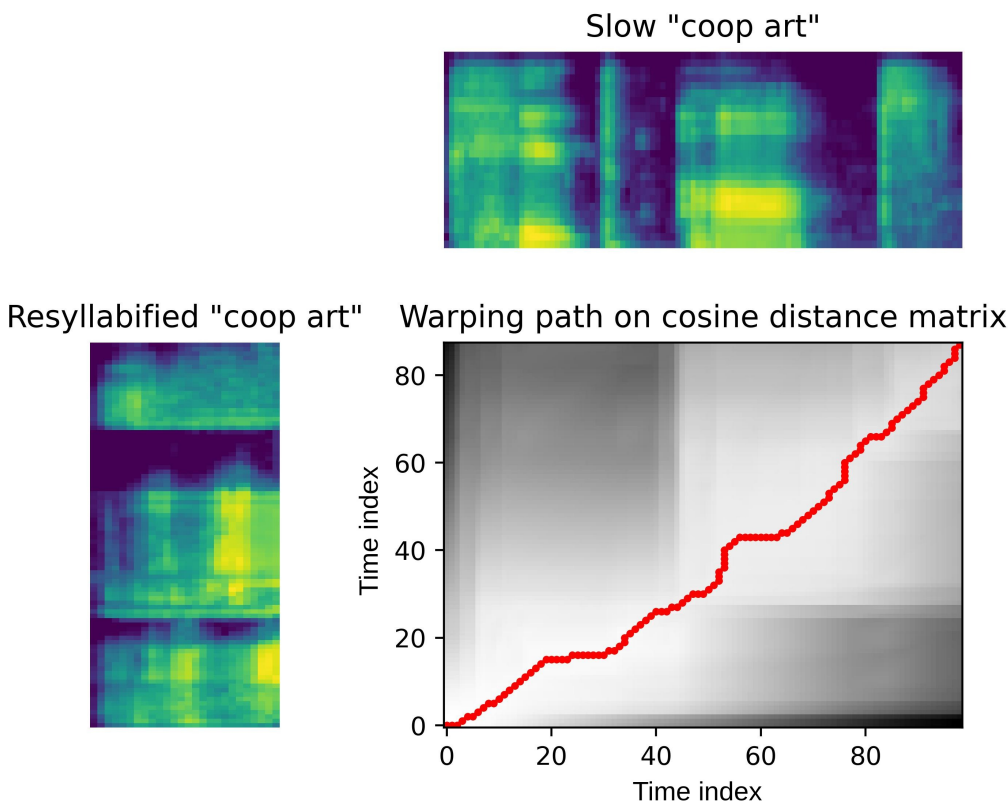
355

356 FIG. 5. Model architecture for the resyllabification classifier. The figure
 357 shows the tensor dimensions for a batch size of 1. The box sizes reflect
 358 tensor shapes, as annotated above each box. The depth, height and width of
 359 the boxes are not to scale and is for illustration purposes only.

360 The trained models were used to classify tokens from the normal speech
 361 rate condition for each speaker. If a coda sequence was misclassified as its
 362 onset counterpart (e.g. “coop art” classified as “coo part”), we categorised it
 363 as resyllabified.

E. Dynamic time warping analysis

Dynamic time warping (DTW) was used to measure how similar the NN-resyllabified and non NN-resyllabified tokens were in relation to the onset or coda conditions in the slow speech rate condition. DTW has been demonstrated to be effective at measuring similarity between sequences such as acoustic signals. For example, it has been widely used for speech recognition (Sakoe & Chiba, 1978; Zhang et al., 2014), as well as other applications such as bird song recognition (Kogan & Margoliash, 1998), speech segment clustering (Lerato & Niesler, 2019), and accent quantification (Bartelds et al., 2020). The DTW algorithm is illustrated in Fig. 6. First, a cost matrix is computed by measuring the distance between the feature vectors (in this case we used mel-spectrograms) between two sequences at each time step. We used cosine similarity for the calculation of distance, as it is not affected by the magnitude of spectral energy, i.e. frequency decibels (e.g. the same recording played at different volumes would measure 0 in cosine distance but not Euclidean distance). The lower right heatmap in Fig. 6 shows the cosine distance between the mel-frequency vectors in the two sequences at all time steps. DTW works by finding the path in the distance matrix that result in the lowest cumulative distance (i.e. cost). Therefore, the DTW distance between the two sequences in Fig. 6 is the sum of the distance values through the warping path shown by the red line.



386

387 FIG. 6. Demonstration of the DTW algorithm. The dotted line shows the
 388 dynamic warping path. The spectrograms are mel-spectrograms of the
 389 tokens “coop art” (bottom left) and “coop art” (top). The pixel intensity in
 390 the lower right heatmap represent feature distances at each time step
 391 between the two spectrograms.

392 Using DTW, we can compute the similarity between word sequences, while
 393 minimising the effect of speech tempo. For this study, we calculated the
 394 distances between the NN-resyllabified as well the the non NN-resyllabified
 395 coda sequences and their onset and coda counterparts in the same group
 396 from the slow rate condition (e.g. NN-resyllabified “coop art” vs. slow “coo
 397 part”, “coo Pete” or NN-resyllabified “coop art” vs. slow “coop art” and

398 “coop eat”). Note that since the vowel contrast is constant between the
399 distance comparisons, it should not confound the analysis.

400 The DTW analysis was used to compare the similarities between the NN-
401 resyllabified sequences and the onset and coda sequences in the slow
402 condition. In addition, a parallel DTW analysis was conducted for the non
403 NN-resyllabified (correctly classified normal rate coda sequences) to assess
404 whether they are more similar to their canonical form.

405 **F. Detecting V_2 information in the intervocalic consonant**

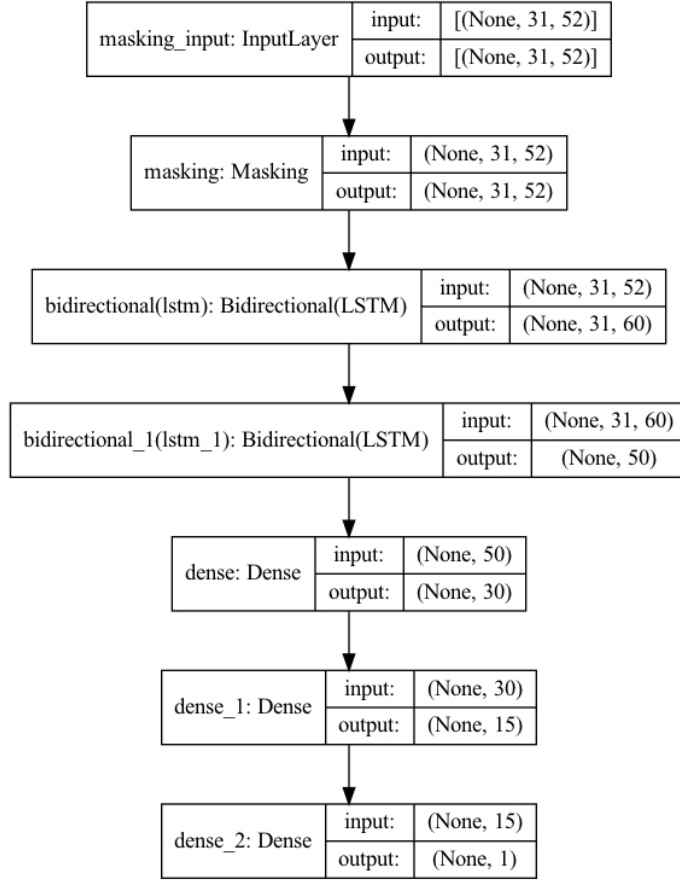
406 As illustrated in Fig. 3, the researcher manually segmented the canonical
407 acoustic intervals from the intervocalic consonant or the first cluster
408 component (i.e. nasal murmur for /m/, aspiration for /p/ and frication for /s/),
409 which were used to investigate the articulatory alignment of the consonant
410 and the following vowel. The segmented intervals differ in terms of
411 articulatory meaning between groups, as aspiration correspond to the
412 consonantal release gesture and the other two correspond to consonantal
413 closures. This difference should have an impact on the amount of vowel
414 information detected in each group. Similar to methods used in Tilsen
415 (2020), Tilsen et al. (2021) and Liu and Xu (2021), to detect vowel
416 information in the segmented intervocalic C, we trained a simple recurrent
417 neural network to predict the second vowel identity between contrastive
418 pairs (e.g. NN-resyllabified “coop art” vs. NN-resyllabified “coop eat”). Liu
419 and Xu (2021) showed that for tautosyllabic C_nV , binary classifiers are able

420 to detect vowel information in the acoustic intervals of onset C, such as
421 during frication or lateral murmur.

422 For each minimal pair, tokens from all 8 speakers were used. From the
423 normal speech rate condition, only the NN-resyllabified tokens and the true
424 onset tokens were examined. According to results from the neural network
425 classifiers, not all coda tokens were NN-resyllabified, which gave rise to the
426 possibility of accuracy scores from the onset conditions being higher than
427 the NN-resyllabified codas, due to having significantly more training data.
428 For example, a speaker resyllabified 5 out of 10 repetitions of “coop art”
429 and “coop eat”, which would result in 10 samples in total for the neural
430 network, whereas 20 samples are available for the onset condition (i.e. 10
431 repetitions of “coo part” and “coo Pete”). Therefore, we balanced the
432 sample sizes between the two conditions by randomly sub-sampling the
433 onset condition for each speaker to match the number of NN-resyllabified
434 ones. For instance, if a speaker resyllabified 5 out of 10 repetitions of “coop
435 eat”, only 5 random selections of “coo Pete” were used from this speaker for
436 training the binary classifier.

437 The classifiers were bi-directional recurrent neural networks with Long
438 Short-Term Memory (LSTM) units (Soltau et al., 2016). The network details
439 are shown in Fig. 7. The hyperparameters were tuned with data from the
440 pilot study using grid search, and details can be found in Table III in the
441 Appendix section. The segmented tokens were converted into mel-

442 spectrograms with 26 filter banks, with 0.025 s as the window length and
443 0.005 s as the hop length. Before training, all the spectrograms were
444 padded to the same length as the longest one. As Fig. 7 shows, masking
445 was applied in the input layer, which tells the model to ignore the padded
446 duration. Due to the absence of CNN, we included delta coefficients (i.e.
447 first order differentials) to aid model performance, which resulted in a 52
448 dimensional vector at each time step. The data were split into training and
449 testing splits with the ratio of 8:2. We randomly shuffled the data for each
450 minimal pair and trained a model from scratch 80 times and reported the
451 accuracy distribution on the testing sets. The motivation behind examining
452 an accuracy distribution is to avoid the issue of accidental above chance
453 performance, which could arise with small datasets (Combrisson & Jerbi,
454 2015; Ojala & Garriga, 2009).



455

456 FIG. 7. Model architecture of the binary classifiers. The tensor shapes are

457 denoted on the right of each box.

458 **1. Bayesian analysis**

459 To test the amount of vowel information in the acoustic signal, we used

460 Bayesian analysis with beta likelihood to model the effect of syllable

461 structure (i.e. onset vs. coda) on model accuracy. A conventional non-

462 significant result cannot be used to validate a null hypothesis, as it only

463 suggests a failure to reject it. The advantage of using Bayesian statistics is

464 that it simply tells us which model is more supported by the evidence in the

465 data, and the models do not need to be nested. The motivation behind using

466 beta regression is due to the nature of accuracy rate being bounded
 467 between 0 and 1. Beta regression assumes that the data generating process
 468 can be modelled by a beta distribution (Balakrishnan & Nevzorov, 2003),
 469 where the distribution can be parameterised with the mean-precision (μ - ϕ)
 470 parameters, where ϕ is analogous to the inverse of data dispersion. Since Y
 471 $\sim \text{Beta}(\mu, \phi)$, beta regression presumes that the mean μ of the response
 472 given the predictor X is linear on the logit transformed scale (Douma &
 473 Weedon, 2019). In other words, in a beta regression model, the dependent
 474 variable can be mapped from the bounded space $[0, 1]$ to unbounded real
 475 numbers with a link function (most commonly the logit function), where an
 476 ordinary linear regression can be used to model the logit transformed data.
 477 During Bayesian estimation of the posterior distribution of the model
 478 parameters, the likelihood function with the μ - ϕ parameterisation is:

$$479 \quad f(y; \mu, \phi) = \frac{\Gamma(\phi)}{\Gamma(\mu\phi)\Gamma((1-\mu)\phi)} y^{\mu\phi-1} (1-y)^{(1-\mu)\phi-1} \quad (1)$$

480 and:

$$481 \quad \mu = \text{logit}^{-1}(X\beta) \quad (2)$$

482 Γ is the Gamma function, μ is the inverse logit transformed model
 483 prediction, y is the observed data bounded between 0 and 1, and ϕ is the
 484 precision parameter. Note that model predictions are mapped back to the
 485 bounded space with the inverse logit function. Our accuracy data contains
 486 values equal to one. Therefore, the one-inflated beta distribution is needed,

487 which produces a mixture density (Ospina & Ferrari, 2012). The likelihood
 488 function using the one-inflated beta distribution incorporates a new
 489 parameter α :

$$490 \quad f(y; \alpha, \mu, \phi) = \begin{cases} (1-\alpha)f(y; \mu, \phi) & (0 < y < 1) \\ \alpha & (y = 1) \end{cases} \quad (3)$$

491 To construct beta regression models with Bayesian analysis with the one-
 492 inflated beta distribution for the likelihood function, we defined a custom
 493 response distribution with the brms package in R³. Weakly informative
 494 Gaussian priors ($\beta \sim N(0, 5^2)$) were used as the priors for the regression
 495 coefficients. The half Cauchy distribution was used for ϕ ($\phi \sim \text{Cauchy}[0,$
 496 $5^2]$), and the beta distribution for α ($\alpha \sim \text{Beta}(0.5, 8)$). Note that model
 497 coefficients do not need to be bounded in any way, as model output is
 498 transformed with the inverse logit function into the bounded space.

499 Bayes Factors (BF) were used for model comparison (Dienes, 2016; Liu et
 500 al., 2022; Stone, 2013). There is controversy regarding using BF to
 501 substitute for null hypothesis testing (Gelman et al., 2013). However, BF is
 502 used here to compare which model is more likely given the evidence (i.e.
 503 the data), rather than the likelihood of the observed effect being due to
 504 chance, as is the case in null hypothesis testing (Morey et al., 2016;
 505 Wagenmakers et al., 2016). Other popular methods such as the Bayes leave-
 506 one-out (LOO) analysis show limitations when the ground truth is consistent
 507 with the null hypothesis. Gronau and Wagenmakers (2019) demonstrates

508 that when the number of observations consistent with the simpler model
509 (i.e. H_0) grows larger, LOO's support for it reaches an upper bound, and this
510 bound can sometimes be very modest. It was also shown that depending on
511 the prior distribution, as more H_0 consistent data is added, LOO's support
512 for H_0 can decrease. Therefore, to avoid potential bias towards the more
513 complex model, we use BF for model comparison.

514 If BF_0 (the BF indicating evidence for H_0 over H_1) is between 0 and 1/10, the
515 data strongly supports H_1 over H_0 . Conversely, if BF_0 is larger than 10, there
516 is strong evidence for the null hypothesis (Jeffreys, 1961; Biel & Friedrich,
517 2018; Dienes, 2014; Harms & Lakens, 2018; Lakens et al., 2020;
518 Schönbrodt & Wagenmakers, 2018; Lee & Wagenmakers, 2014).

519 For each speech rate condition, a full model was constructed with the main
520 effects of syllable structure (onset vs. coda for the slow rate and onset vs.
521 NN-resyllabified coda for the normal rate) and group. The null model was
522 constructed with group as the only main effect. We also tested whether the
523 effect of syllable structure differed between item groups, by including an
524 interaction term.

525 **G. Duration analysis of NN-resyllabified and canonical onset** 526 **consonants**

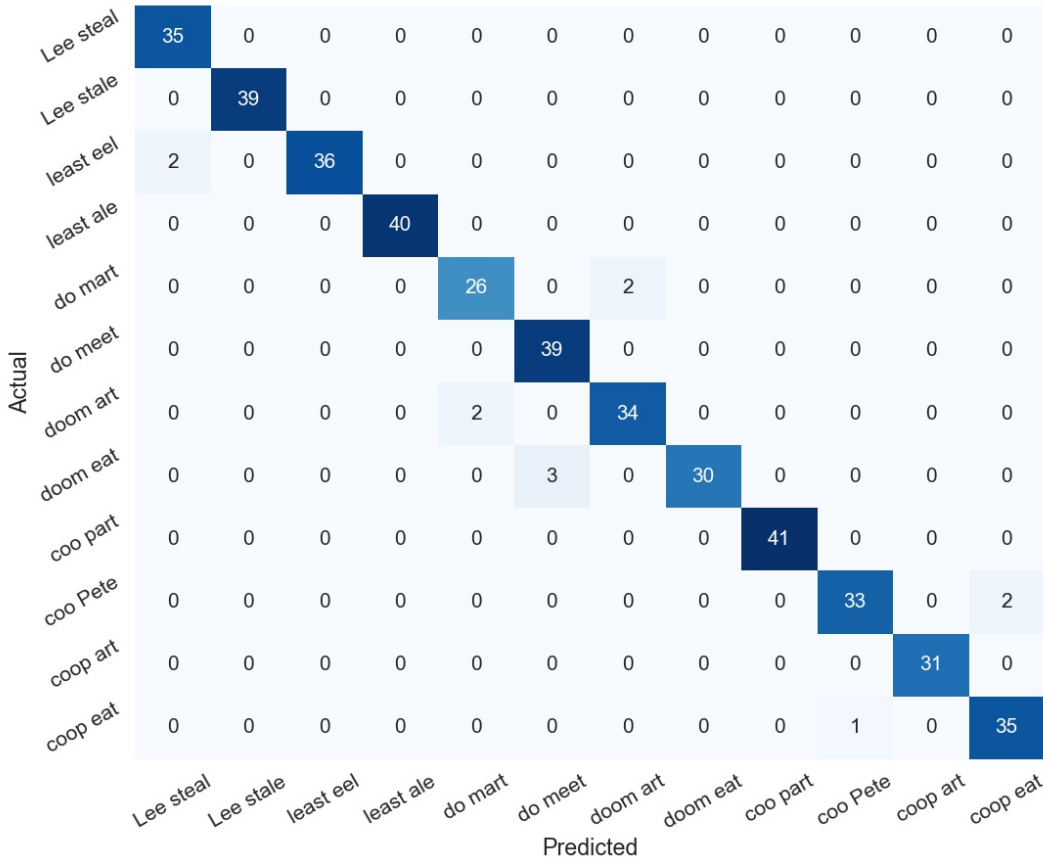
527 Although resyllabified sequences may have become similar to their onset
528 counterparts in terms of spectral pattern, there is evidence that resyllabified
529 codas retain their underlying coda status through duration (Gao & Xu,

2010; Lehiste, 1960). Specifically, the durations of the resyllabified consonants are shorter compared to the canonical onsets. To test whether duration differs between the two, the same acoustic intervals from the previous section were used. Bayesian analysis with *linear* regression was used to determine if duration of the acoustic interval was affected by syllable affiliation (i.e. genuine onset vs. NN-resyllabified coda). Duration was used as the dependent variable and item group and syllable affiliation were used as the predictor. The likelihood function used the normal Gaussian distribution. For the regression coefficient priors, we used weakly informative Gaussian prior ($\beta \sim N(0, 5^2)$), and for the sigma prior we used the half Cauchy distribution ($\sigma \sim \text{Cauchy}[0, 5^2]$).

III. Results

A. Resyllabification classifiers

Fig. 8 shows the model performance of the word sequence classifiers. Since we trained a model for each speaker separately, the result in Fig. 8 was calculated by summing over each speaker's confusion matrix. As shown, the classifiers achieved near ceiling accuracy on the test split for the slow speaking rate, indicating that the models could distinguish the word sequences very well.

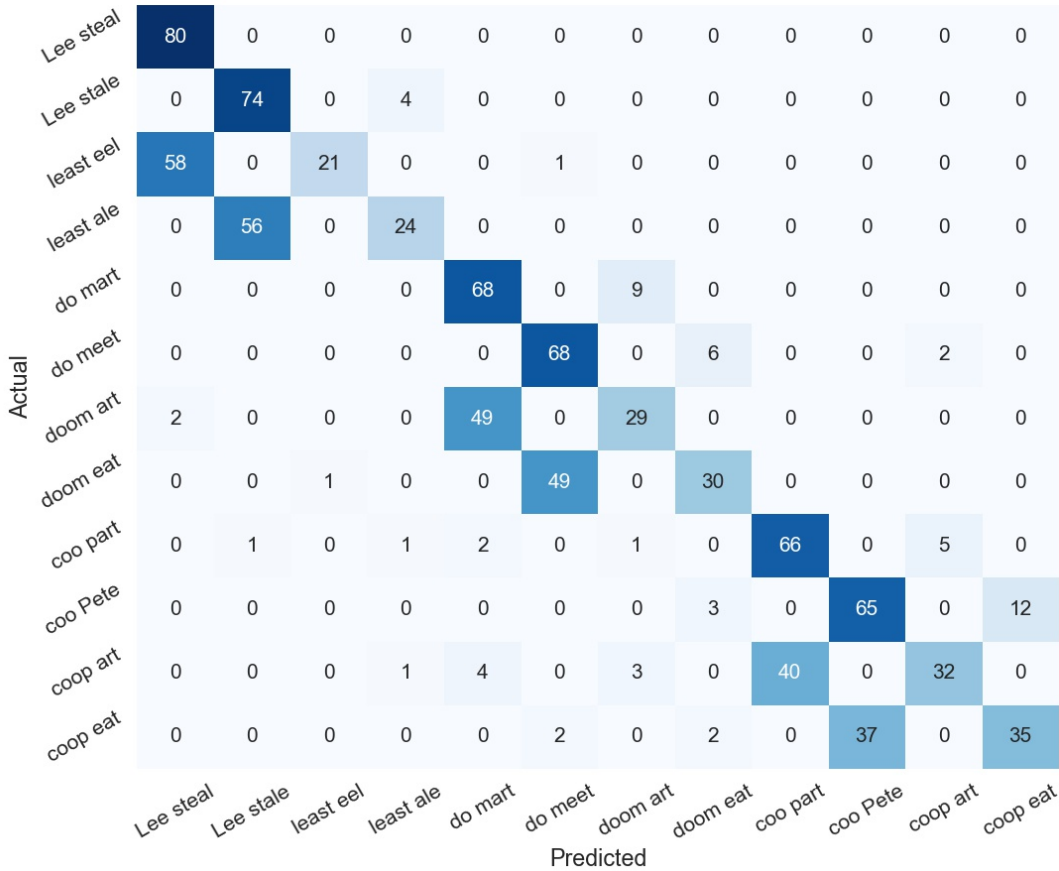


549

550 FIG. 8. Confusion matrix of model performance on the testing split of the
 551 slow speech rate. This is an element wise summation of all the speakers’
 552 confusion matrices. The colour intensity of tiles reflects numeric value.

553 Fig. 9 shows the model performance on the normal speaking rate by
 554 summing over the results from all the speakers. Table IV list the accuracy
 555 rate for the onset, coda and all sequences. As can be seen, most of the onset
 556 sequences were classified correctly. Thus, the classifiers trained on the slow
 557 speaking rate data also did well on the onset conditions spoken at a faster
 558 rate, such as “Lee steal” or “Lee stale”. In the coda condition, the classifiers

559 misclassified a large portion of the sequences as their onset counterpart,
 560 such as classifying “least eel” as “Lee steal”. These misclassified sequences,
 561 presumably due to resyllabification, are examined in detail later.



562

563 FIG. 9. Confusion matrix of model performance on the normal speech rate.
 564 This is an element wise summation of all the speakers’ confusion matrices.
 565 The colour intensity of tiles reflects numeric value.

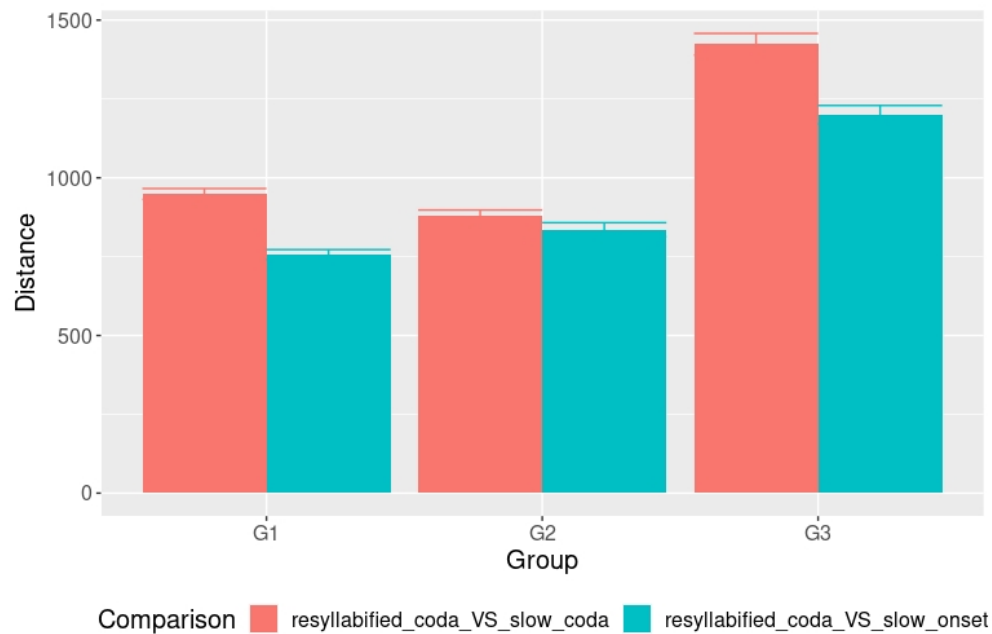
566 TABLE IV. Accuracy summary for the normal speech rate tokens.

Coda	0.36
Onset	0.90
Overall	0.63

567

568 **B. DTW analysis**

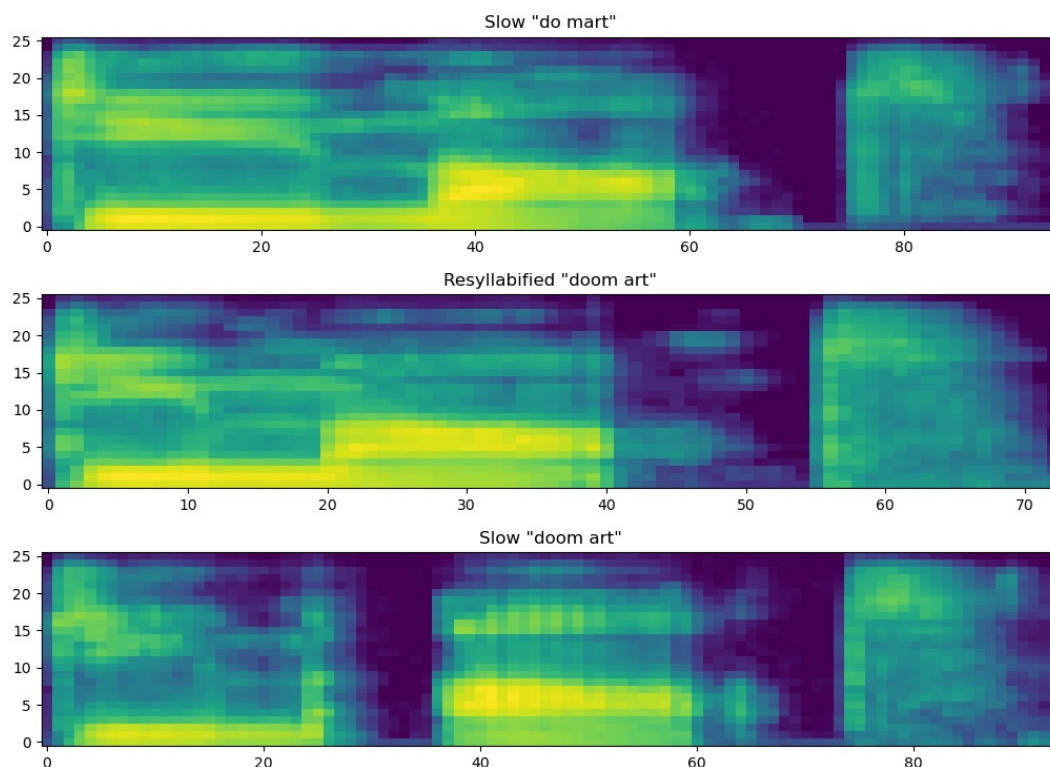
569 Fig. 10 shows a bar graph of the cosine distance between the NN-
570 resyllabified tokens and the slow tokens. The NN-resyllabified sequences
571 were only compared to slow sequences in the same group. The figure shows
572 that, when minimising the effect of speech tempo, NN-resyllabified words
573 such as “least eel” is more similar to its canonical onset counterpart “Lee
574 steal” than to its non-resyllabified version. In other words, when comparing
575 the NN-resyllabified condition with the slow onset condition, the cosine
576 distance is smaller than when comparing with the slow true coda condition.



577

578 FIG. 10. DTW cosine distance between resyllabified normal rate sequences
 579 and slow sequences. The error bars represent 95% of the confidence
 580 interval. G1 - “least eel”, “least ale”, “Lee stale”, “Lee steel”; G2 - “doom
 581 art”, “doom eat”, “do mart”, “do meet”; G3 - “coop art”, “coop eat”, “coo
 582 part”, “coo Pete”.

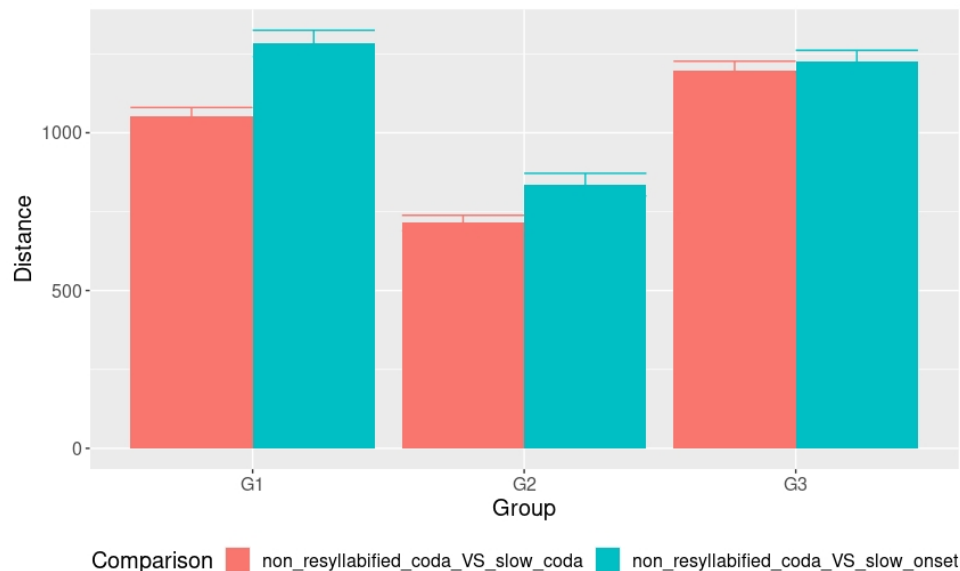
583 The result from the DTW analysis can be reflected by the spectrograms in
 584 Fig. 11. “doom art” in the middle of Fig. 11 was classified as “do mart” by
 585 the neural network in the previous section, therefore we treated it as a
 586 resyllabified token. The NN-resyllabified “doom art” appears to be more
 587 similar to the canonical onset version “do mart” in the top panel. The
 588 bottom panel shows “doom art” spoken in the slow condition, likely with a
 589 glottal stop at the beginning of the second syllable “art”.



590

591 FIG. 11. Mel-spectrograms of three word sequences from one speaker.

592 Fig. 12 shows the DTW cosine distance between correctly classified normal
 593 rate coda tokens and the slow tokens. The opposite trend from Fig. 10 can
 594 be observed: the non NN-resyllabified sequences are more similar to their
 595 canonical coda form in the slow rate condition, which support the prediction
 596 that correctly classified coda tokens likely have not been resyllabified,
 597 unlike their misclassified counterparts.



598

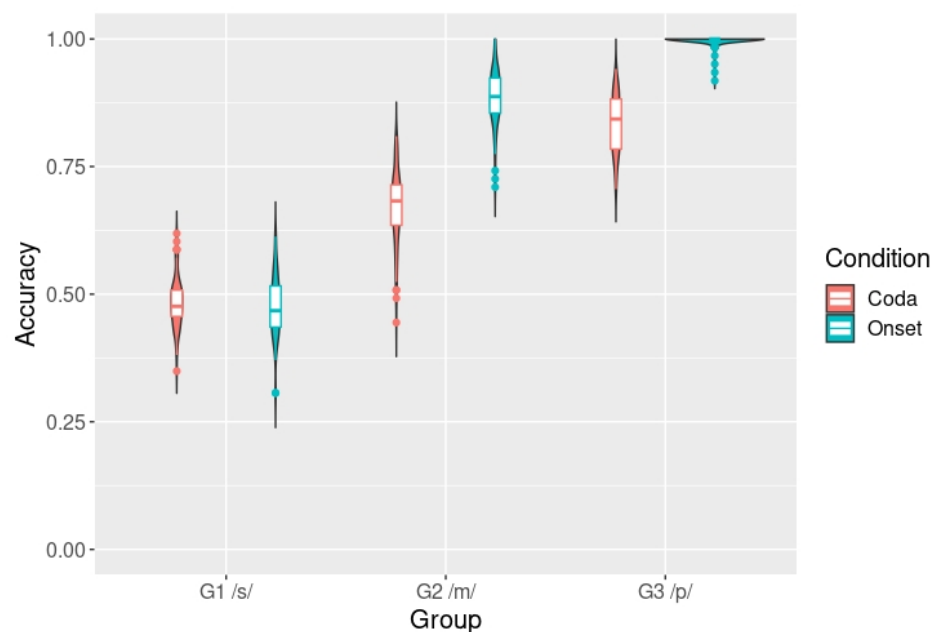
599 FIG. 12. DTW cosine distance between non NN-resyllabified normal rate
600 sequences and slow sequences. The error bars represent 95% of the
601 confidence interval. G1 - “least eel”, “least ale”, “Lee stale”, “Lee steel”; G2
602 - “doom art”, “doom eat”, “do mart”, “do meet”; G3 - “coop art”, “coop eat”,
603 “coo part”, “coo Pete”.

604 C. Intervocalic consonant alignment analysis

605 1. Results for slow speech rate

606 With the consonant intervals described in Section II E, we trained 80 neural
607 networks for each vowel minimal pair in Table I and obtained an accuracy
608 distribution from the test set. Fig. 13 shows the accuracy rate from the slow
609 speech rate condition. As the figure shows, for /s/ frication in the
610 intervocalic cluster (i.e. G1), the vowel classification accuracy is around
611 chance, indicating that little to no vowel information was picked up by the
612 binary classifier in the frication of /s/ for both the onset (e.g. “Lee stale”)

613 and coda conditions (e.g. “least ale”). For G2, the intervocalic /m/ contains
 614 more detectable vowel information as the onset of the second syllable, and
 615 less so when it is the coda of the first syllable. Similar trends can be
 616 observed for G3, although with overall higher accuracy – the binary
 617 classifier performs better when /p/ is the onset of the second syllable.

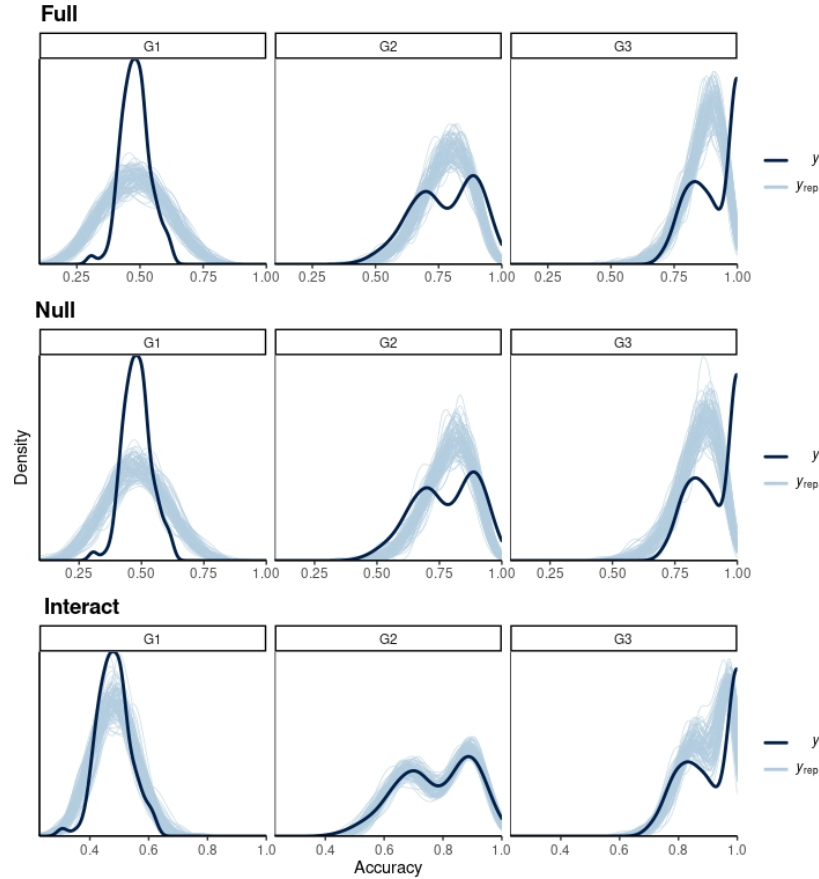


618

619 FIG. 13. Vowel classification accuracy by group from the slow speech rate
 620 condition. G1 – “least eel”, “least ale”, “Lee stale”, “Lee steel”; G2 – “doom
 621 art”, “doom eat”, “do mart”, “do meet”; G3 – “coop art”, “coop eat”, “coo
 622 part”, “coo Pete”.

623 To test hypothesis via model comparison, we use the Bayes Factor, which
 624 can offer support for a model based on the observed data (Dienes, 2014,
 625 Harm & Lakens, 2018). The posterior distributions of the model parameters
 626 are not very informative as predictions need to be transformed with the

627 inverse logit function, and their details are included as supplementary
628 materials⁴. Therefore, the predicted distribution from 100 random samples
629 is shown in Fig. 14. As the figure shows, the model with an interaction term
630 shows the best predictive power. BF_0 was very close to zero (i.e. BF_1 is
631 larger than 10). Therefore, the data indicate that the alternative model, i.e.
632 onset and coda conditions are different, is highly more likely, because
633 model accuracy differs greatly. We also constructed a model with an
634 interaction effect between item group and syllable structure. $BF_{\text{interaction}}$ (the
635 BF indicating support for the interaction model over the full model) is larger
636 than 10, which provides strong support for the interaction model. To
637 conclude, the data shows strong evidence for the effect of syllable structure,
638 which differs greatly between groups. In other words, there is robust effect
639 of syllable structure for G2 and G3, but likely not for G1.



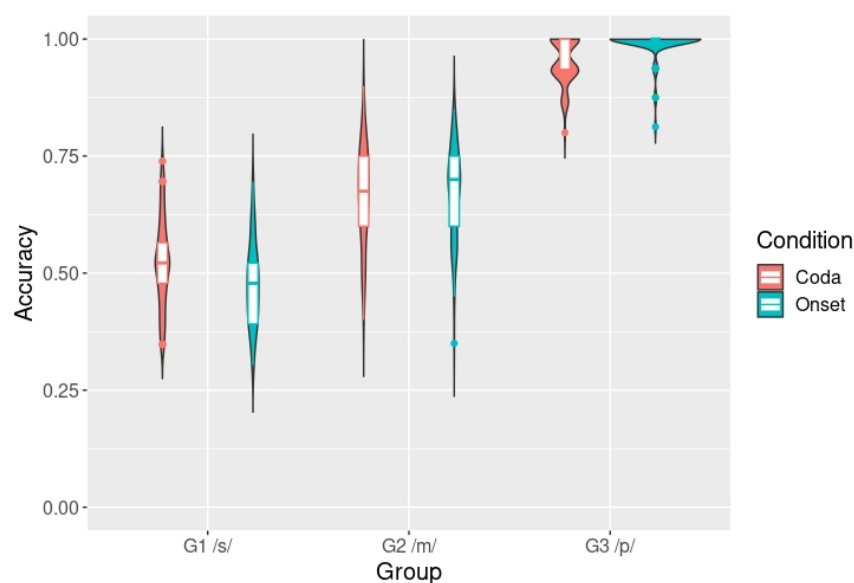
640

641 FIG. 14. Model predictions against 100 random samples for the slow rate,
 642 where y refers to the observed data and y_{rep} refers to predictions. The
 643 columns correspond to item groups and the rows correspond to model type.

644 2. Results for normal speech rate

645 The accuracy distributions from the normal speech rate condition are shown
 646 in Fig. 15. Note that the coda condition only contained NN-resyllabified
 647 sequences. Fig. 15 shows that the amount of vowel information detected
 648 during the acoustic consonantal intervals (e.g. /s/ frication in “Lee stale”)
 649 was very similar between the NN-resyllabified coda and onset sequences.
 650 The item group wise trends are similar to the slow rate condition in Fig. 13.

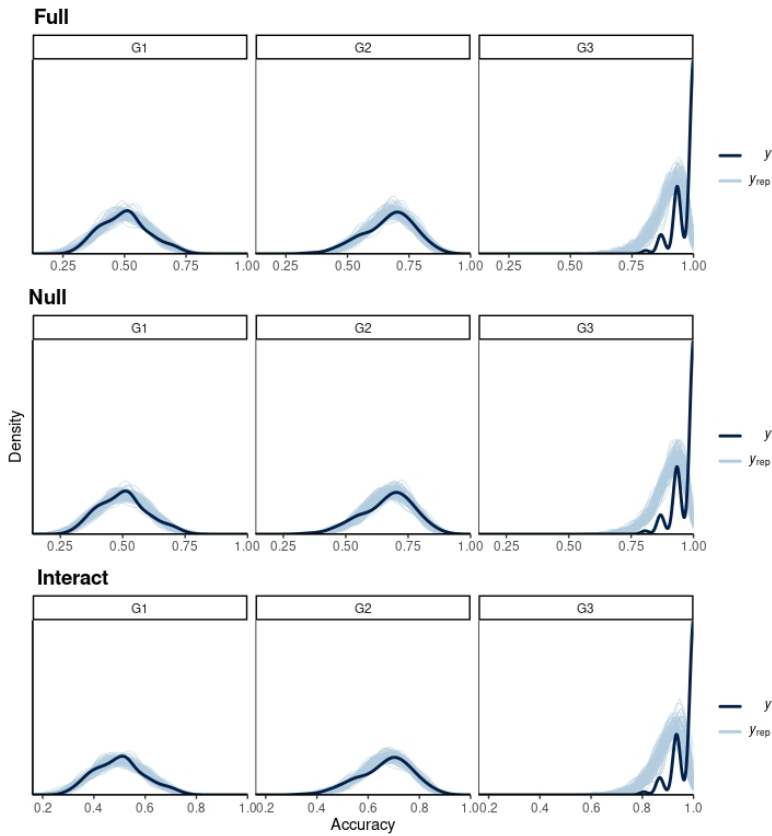
651 The aspiration from the plosive onset /p/ contains the most vowel related
652 energy, and the nasal murmur from /m/ contained enough vowel information
653 for the classifier to perform above chance. For /s/ in G1, the accuracy
654 distributions are centered at chance level (i.e. 50%), indicating that little to
655 no vowel information was detected by the binary classifiers during the
656 frication intervals.



657
658 FIG. 15. Vowel classification accuracy by group from the normal speech
659 rate condition. The coda condition here refers to the NN-resyllabified coda
660 sequences in the normal speech rate condition. G1 - “least eel”, “least ale”,
661 “Lee stale”, “Lee steel”; G2 - “doom art”, “doom eat”, “do mart”, “do meet”;
662 G3 - “coop art”, “coop eat”, “coo part”, “coo Pete”.

663 The predicted distributions from the Bayesian analysis results are shown in
664 Fig. 16. The posterior distributions of model parameters can be found in the
665 supplemented materials⁵. Visually, the predicted distributions do not differ

666 too much from one another. BF_0 was larger than 10, signifying that the data
 667 provides more support for the null model. Fig. 15 indicates that model
 668 accuracy might differ slightly between the NN-resyllabified coda and the
 669 onset sequences for G1. In other words, there might be an interaction
 670 between the effect of syllable structure and group. $BF_{interaction}$ (the BF
 671 indicating support for the interaction model over the null model) is smaller
 672 than 1/10, therefore, there is little to no evidence suggesting that accuracy
 673 differs between onset and NN-resyllabified coda tokens for G1.



674
 675 FIG. 16. Model predictions against 100 random samples for the normal rate,
 676 where y refers to the observed data and y_{rep} refers to predictions. The
 677 columns correspond to item groups and the rows correspond to model type.

D. Duration of intervocalic consonants

The duration of the acoustic intervals for the canonical and NN-resyllabified onsets are shown in Fig. 17. Congruent with previous findings (Gao & Xu, 2010; Lehiste, 1960), NN-resyllabified codas are shorter than the canonical onsets. Predictions of the Bayesian analysis are shown in Fig. 18, and the parameter posterior distributions are included as supplemented materials⁶. The effect of syllable structure was estimated to be around 0.01 ($\mu = 0.008$ [0.005, 0.012]). BF_0 is smaller than 1/10, which indicates that duration differs between syllable structures.

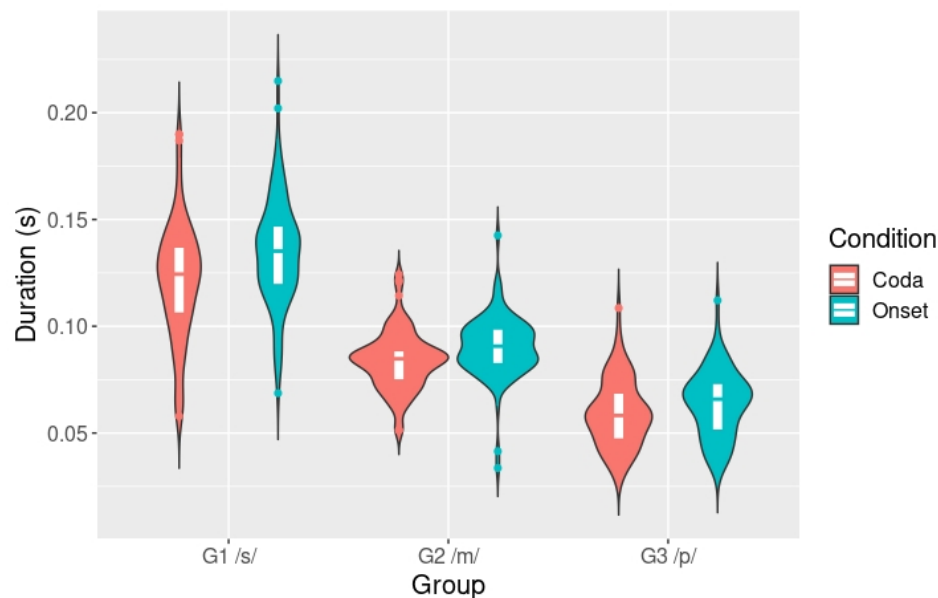


FIG. 17. Duration of onset and NN-resyllabified consonants from the normal speaking rate condition.

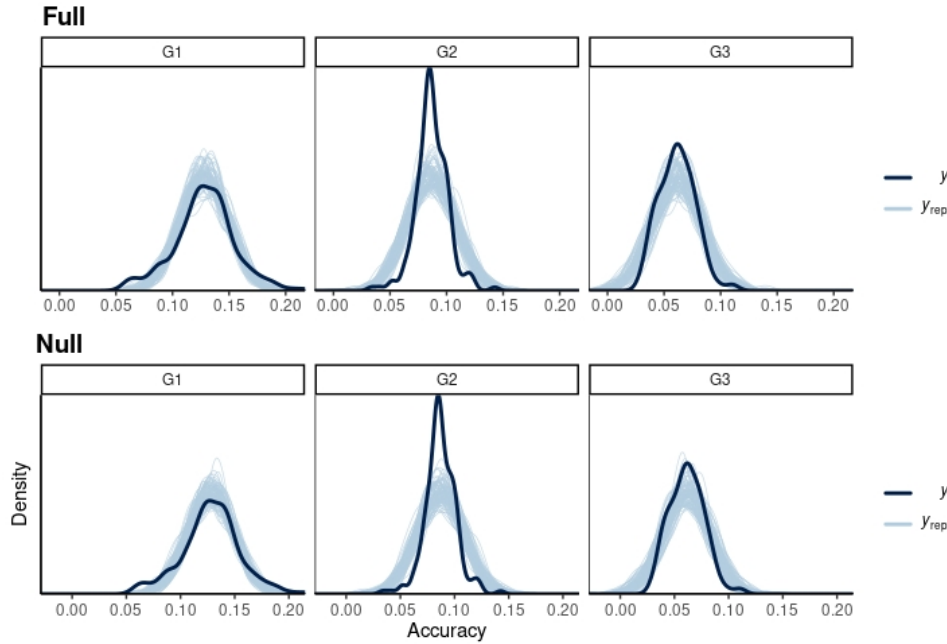


Fig. 18. Model predictions against 100 random samples for the duration results, where y refers to the observed data and y_{rep} refers to predictions. The columns correspond to item groups and the rows correspond to model type.

IV. Discussion

Previous debates on the phenomenon of resyllabification have mainly relied on phonotactic analysis, listener judgment or phonetic properties such as voicing and aspiration. In this study we tested an alternative approach that examines articulatory coordination, and coarticulation, as reflected in the spectral patterns, using machine learning models with acoustic data. The findings have offered a new perspective on the nature of resyllabification.

A. Overall findings

The results of computational analysis have largely confirmed the two predictions laid out in the introduction. The deep learning models trained on slow speech rate data misidentified coda sequences by classifying them as their onset counterparts, and DTW analysis showed that for all three consonants (i.e. /st/, /p/ and /m/), the sequences identified as resyllabified were more similar to their onset versions than the original coda versions. Moreover, the correctly classified sequences are more similar to their canonical coda version, which indicate that they likely have not undergone resyllabification. Therefore, the first prediction — codas in the NN-resyllabified sequences spectrally resemble canonical onsets more than their canonical coda version, was supported. The results from the binary classifiers confirm the second prediction by showing that there was a similar amount of vowel information detected in the NN-resyllabified onsets and canonical onsets, but not between the true codas and onsets from the slow condition. This suggests that the underlying articulation was alike between the NN-resyllabified and canonical onsets. Therefore, the results confirm previous findings of resyllabification in English (de Jong, 2001; Gao & Xu, 2010; Stetson, 1951). In connected speech, resyllabification can happen when a coda consonant is followed by a vowel initial syllable, and it applies to both singleton consonants and consonant clusters. The coda status of the NN-resyllabified consonants, however, seem to be partially retained through duration: Resyllabified codas are shorter compared to

725 canonical onsets. This is consistent with the findings of Lehiste (1960) and
726 more recently Gao and Xu (2010). Whether or not listeners can perceive the
727 durational cues, however, need to be tested in future studies. Furthermore,
728 future studies can investigate the effect of resyllabification and syllable
729 position on consonant duration by examining both NN-resyllabified and non
730 NN-resyllabified consonants.

731 It is also interesting to note the relation between resyllabification and
732 speech rate. When syllable duration is around 350 ms in the current study,
733 the rate of inferred resyllabification already reaches above 50%. At 2.86
734 syllables per second, this speech rate is rather slow, compared to the typical
735 normal articulation rate of 5-7 syllables per second in connected speech
736 (Eriksson, 2012; Tiffany, 1980). But this is consistent with the finding of de
737 Jong (2001) that resyllabification start to take place as speech rate
738 increases to around 350 ms per syllable, and resyllabification rate
739 approaches 100% at 150 ms per syllable. The implication is that the
740 tendency for resyllabification must be very strong so that it would be
741 difficult to avoid at normal speech rate.

742 The finding of resyllabification align with the syllable model shown in Fig. 1
743 based on which the predictions illustrated in Fig. 2 were derived. That is,
744 once a coda consonant is resyllabified as the onset of the next syllable, as
745 determined by the deep learning model and DTW analysis, its articulation is
746 overlapped with the vowel of the next syllable, as determined by the binary

747 classifiers. This is consistent with the recent finding that the movements
748 towards the vowel and onset C are synchronised at syllable onset (Liu et al.,
749 2022; Liu & Xu, 2021; Xu et al., 2019), which is denoted by the rime and
750 onset tiers in Fig. 1.

751 **B. Coarticulation resistance and dimension-specific sequential**
752 **target approximation (DSSTA)**

753 CV synchronisation does not mean that vowel information is always
754 detectable from the syllable onset or at the same time point, however,
755 partly due to *coarticulation resistance*, i.e. the ability of a segment to
756 restrain coarticulatory effects from adjacent segments (Bladon & Al-
757 Bamerni, 1976; Recasens, 1984). Recasens (1984) proposes that the degree
758 of coarticulation resistance is dependent on the amount of constraint that a
759 consonant or vowel places on the tongue body. Xu (2020) further proposes
760 that the phenomenon is a mechanism that resolves the articulatory conflicts
761 between consonants and vowels when they both involve the same
762 articulator while being co-produced to achieve C-V co-onset (Fig. 1).

763 According to this mechanism, namely, *dimension-specific sequential target*
764 *approximation mechanism*, different (e.g. vertical or horizontal) dimensions
765 of an articulator can be engaged in executing only a single target, which is
766 either consonantal or vocalic, during C-V coproduction. This mechanism
767 maximises the degree of C-V synchronisation while allowing individual
768 articulator dimensions to be engaged in only sequential target
769 approximation movements, i.e. without gestural blending (Saltzman &

770 Munhall, 1989) given its computational difficulty (Tilsen, 2019). The
771 following discussion will offer an account of the differences in the detected
772 vowel information in the present results that includes DSSTA as a critical
773 mechanism.

774 The amount of detectable vowel information in the consonant interval
775 follows the order of Group 1 (/s/) < Group 2 (/m/) < Group 3 (/p/). This order
776 may result from two different sources. The first, which is more obvious, is
777 the differences in their relative timing. The frication in Group 1 and nasal
778 murmur in Group 2 both correspond to the articulatory closure of the
779 consonants, whereas the aspiration in Group 3 corresponds to the
780 articulatory release, which occurs after the closure. This could partially
781 explain why more vowel information was detected in Group 3 than in the
782 other two groups. The second source is coarticulation resistance due to
783 DSSTA. The consonant /s/ in Groups 1 involves the tongue body to form a
784 groove needed to direct the airflow toward the front teeth (Borden, Harris
785 and Raphael, 2003). The involvement of the tongue body would generate
786 serious coarticulation resistance in /s/ in Group 1 because the horizontal
787 and vertical dimensions of the tongue body are likely both involved in
788 approaching the target of the sibilant (Recasens & Espinosa, 2009). In
789 contrast, the articulation of /m/ in Group 2 requires only lip closure without
790 constraints on the tongue. This would account for the greater amount of
791 detectable vowel information in Group 2 than in Group 1. The lack of tongue
792 involvement in labial consonants is true of /p/ in Group 3 as well. But there,

793 it is added on top of the fact that aspiration, where the binary classification
794 was performed, occurs after the stop closure, thus giving rise to the
795 maximal vowel information detected by the classifier. Note that had one of
796 the syllables in Group 1 contained a rounded vowel such as /u/, DSSTA
797 would predict that vowel information would be better detected, because lip
798 movements are not in direct conflict with the articulation of /s/. This
799 possibility can be tested in future research.

800 **C. Chance level performance of the binary classifier for G1** 801 **sequences**

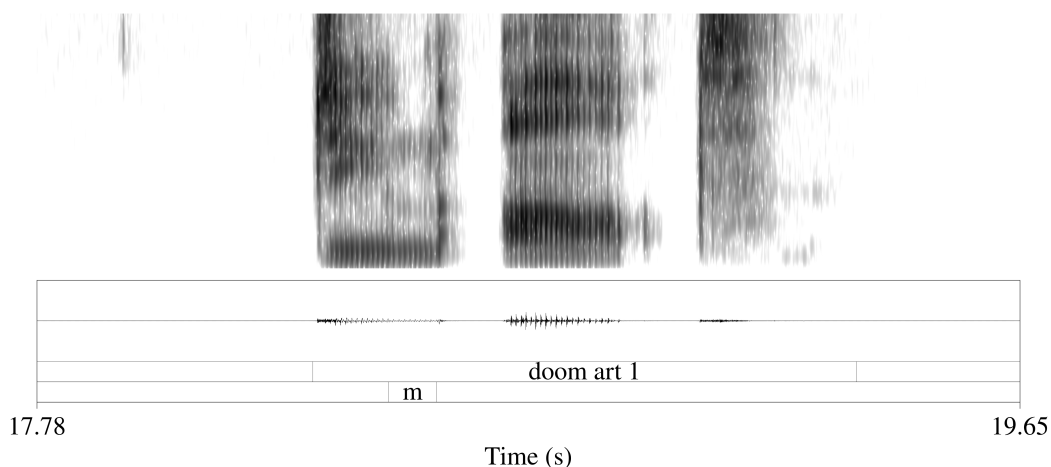
802 The lack of detectable vowel information in /st/ even in normal speech rate
803 may seem to contradict the recent finding that vowel articulation could be
804 detected at the same time as the onset of a consonant cluster (Liu & Xu,
805 2021). That study found that for a minimal triplet such as “slit” vs. “slot” vs.
806 “flot”, the difference between “slit” and “slot” could be detected around the
807 same time as “slot” and “flot”, *before* the frication onset. But we have noted
808 three major differences between Liu and Xu (2021) and the current study.
809 First, Liu and Xu (2021) only looked at clusters such as /sp/ and /sl/, but
810 not /st/ as in the current study. /p/ does not require any tongue movement,
811 thus is less coarticulation resistant than both /l/ and /t/. In terms of /l/ and
812 /t/, both being alveolars, Iskarous et al. (2013) found that /t/ is more
813 coarticulation resistant than /l/ in the vertical dimension for the jaw and the
814 tongue blade. This could be due to the requirement of a full closer for /t/ as
815 a plosive but not for the approximant /l/. /t/ being more coarticulation

816 resistant means that it may have delayed much of the vowel movements.
817 Second, much larger vowel contrasts were involved in Liu and Xu
818 (2021)—/slit/ vs. /slot/ than those in the present study—/steal/ vs. /stale/.
819 The greater the vowel contrast, the greater the magnitude of tongue
820 movement in the articulatory dimensions not essential for the consonant
821 articulation, and the more detectable the vowel information during the
822 frication interval. Third, the target words were produced with a carrier in
823 Liu and Xu (2021), which made the speech more fluent than the isolated
824 word sequences said in the present study. The average speech rate in Liu
825 and Xu (2021) was about 140 ms per syllable, compared to 350 ms per
826 syllable in this study. It is hard to tell, however, if any of these factors is
827 decisive, or all of them jointly contribute to blocking the vowel information
828 from being present in the /s/ frication.

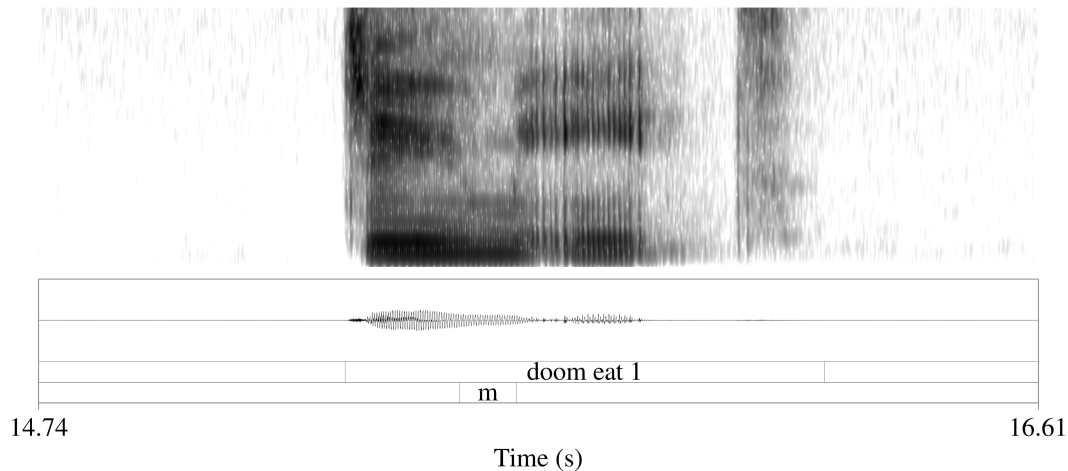
829 **D. Above chance performance of the binary classifier for the slow**
830 **coda sequence in G2**

831 One of the most surprising results of this study is the finding that, as shown
832 in Fig. 13, for the slow speaking rate, there is information of the upcoming
833 vowel in the intervocalic consonants when they are in the coda position of
834 the first syllable (e.g. “doom art”; “coop art”), albeit less than when they are
835 in the onset position. The detection of vowel information in a non
836 resyllabified coda may seem particularly striking given the clear temporal
837 gap or glottalisation between the two syllables, as can be seen in Fig. 19
838 and Fig. 20. But the glottal component, as can be judged both auditorily and

839 spectrally, corresponds to a glottal stop or glottalisation (which is also a
 840 form of glottal stop: Redi & Shattuck-Hufnagel, 2001; Garellek, 2013), that
 841 serves as the onset of the syllable /art/. A glottal stop, just like other stops
 842 such as /b, d, g/, would be fully coarticulated with the following vowel (Xu,
 843 2020), as illustrated in Fig. 2. This means that the target approximation
 844 of /a/ must have started some time well before the glottal closure (Liu et al.,
 845 2022; Xu and Liu, 2007). This can indeed be seen in Fig. 19, i.e. the brief
 846 yet clearly visible labial release after the nasal murmur of /m/, and the F2
 847 transition from “doom” to “eat” during and right before the glottalised
 848 interval in Fig. 20. The high vowel detection rate of around 80% for /p/ and
 849 65% for /m/ means that the vowel target approximation may have started
 850 during (though probably not before) the closure of the coda. Exactly when
 851 during the closure, however, awaits future investigations.



852
 853 FIG. 19. Spectrogram of “doom art” from a male speaker.



854

855 FIG. 20. Spectrogram of “doom eat” from a female speaker.

856 E. Broader implications

857 The finding of a clear tendency toward resyllabification in this study

858 provides further support for the synchronisation model of the syllable (Xu,

859 2020) beyond recent findings (Liu et al., 2022; Liu & Xu et al., 2021).

860 According to the model, there is a strong demand for onset consonants to

861 synchronise (i.e. fully overlap) with the vowel, and a high time pressure

862 against the preservation of coda consonants. This is partially consistent with

863 the maximum onset principle (Pulgram, 1970; Selkirk, 1982), but offers

864 specific articulatory details that can be tested in the acoustic signals as

865 done in the present study. Because the syllable is both essential and highly

866 controversial for theoretical models in linguistics as well as

867 psycholinguistics, the current results may have implications for many

868 broader issues about speech production, but here we focus only on two

869 major ones. The first is about the influential psycholinguistic model of

870 speech production (Levelt et al., 1999), which proposes a step-by-step
871 model of how speech production proceeds from lexical selection to
872 articulation. The results of the present study are relevant for the
873 phonological encoding to articulation stages in the model. The most
874 relevant result is probably the corroboration of previous findings that
875 resyllabification is contingent on local articulation rate: highly likely at
876 normal rate, but optional at slow rate (de Jong, 2001; Stetson, 1951). This
877 means that until local speech rate is known, the articulatory affiliation of
878 coda consonant is undetermined, which would suggest that either syllables
879 retrieved from memory (during phonological encoding) are incomplete in
880 terms of segment affiliation, or the retrieved syllables are reorganised by
881 resyllabification, and that this reorganisation would occur *after* the phonetic
882 encoding stage, just before articulation.

883 The finding of rate-dependency of resyllabification is further relevant to any
884 psycholinguistic model of speech production given the known extensive use
885 of speech timing by linguistic functions. Specifically, local articulation rate,
886 which is jointly determined by syllable duration and pause duration, is used
887 to encode multiple levels of boundary strength (Lehiste, 1972; Klatt, 1976;
888 Nakatani, O'Connor & Aston, 1981; Wagner, 2005; Wang & Xu, 2019). Thus
889 resyllabification is likely a regular variable of connected speech beyond
890 word-level phonetics. In fact, it is likely part of the process of producing
891 connected speech that involves many other phonetic reorganisations,
892 including deletion of intervocalic coda (as opposed to resyllabification in

893 some languages) (e.g. tone sandhi (Chen, 2000), intrusive /r/ (Gick, 1999),
894 and vowel hiatus breakers (Mudzingwa, 2013), etc). There is already
895 evidence that some of these reorganisations may be cognitively real, at least
896 in the case of tone sandhi (Zhang, Xia & Peng, 2015). These phonetic
897 reorganisation tactics could therefore be included in an enhanced
898 psycholinguistic model of speech production, and their cognitive reality
899 could be experimentally investigated.

900 The second broad issue is whether the present results can be interpreted in
901 terms of ambisyllabicity. The original proposal of ambisyllabicity was
902 motivated by the lack of phonetic means to clearly determine syllable
903 boundaries, so the affiliation of intervocalic segments had to rely on
904 phonotactic well-formedness, and for cases where *ill-formed* syllables would
905 occur if an intervocalic consonant can only have a single affiliation, e.g.,
906 *happy, attic, hobby*, the solution is ambisyllabicity, i.e., simultaneously
907 affiliation to both adjacent syllables (Kahn, 1976). Exactly how such double
908 association is realised phonetically, however, has remained unclear. Gick
909 (2003) has proposed that some intervocalic segments, e.g. /l/ and /w/,
910 actually consist of a C-gesture and a V-gesture, which are simultaneously
911 phased to the surrounding syllables, therefore ambisyllabified. The phonetic
912 evidence is in terms of different time delays in the *achievement of the*
913 *respective C and V gestural goals, which differs from the onset alignment*
914 *the current study has examined*. Although the present study is not designed
915 for examining ambisyllabicity, at least one phonetic cue is shown to have

916 the potential to indicate the original coda status of a consonant, namely, the
917 shorter duration of NN-resyllabified coda than the original onset consonant
918 (also c.f. Lehiste, 1960). However, if CV onset coarticulation is considered
919 as the sole indicator, the NN-resyllabified codas are unambiguously
920 overlapped with the following vowel according to the present data.

921 **F. Caveats**

922 Two of the resyllabification classifiers satisfied the early stopping criteria,
923 which meant that their training epochs were determined with the test split
924 rather than the pilot data. This could have slightly inflated the overall
925 accuracy reported for the slow condition in section III A. However, the use
926 of the classifier is to classify normal rate sequences, which is the focus of
927 the study and their accuracy has not been inflated as the normal rate data
928 were not used in any way during training.

929 The possibility of false negatives cannot be completely ruled out regarding
930 the chance level performance of the binary classifier for G1. Providing that
931 upcoming vowel related acoustic information exist during frication, two
932 scenarios could result in false negative detections:

933 1. Chance performance due to chance.

934 2. The neural networks are not powerful enough to detect the subtle
935 difference.

936 The first scenario refers to the opposite of what is described in Combrisson
937 and Jerbi (2015), namely, the model achieved chance performance by
938 chance. This could be due to the randomised nature of the data split and/or
939 model parameter initialisation (not hyperparameters). However, this
940 possibility is accounted for in the current study, by repeatedly training 80
941 classifiers on randomised train and test data and analysing the resultant
942 accuracy distributions. For the second scenario, despite tuning the
943 hyperparameters with data from pilot recordings, the neural network was
944 not tuned for each speaker and consonant type separately. In practice, it is
945 very difficult to construct a perfect network regardless of the type of data in
946 question. Therefore, there is a small possibility that the binary classifier
947 could not detect a difference between groups in G1 due to the lack of
948 robustness. Future studies could incorporate articulatory data, as it might
949 provide more detailed information than acoustic data in the current study
950 (Tilsen, 2020).

951 On the other hand, the possibility of false positives cannot be ruled out
952 either. Providing that the test dataset is large enough, machine learning
953 models cannot always achieve 100% accuracy. The same applies to the
954 word sequence classifiers in this study. This is evident in the results from
955 the slow speech rate in section III A. Although overall accuracy is high,
956 there were still coda sequences classified as their onset counterpart, as well
957 as cases where onset sequences were classified as their coda counterpart.
958 At the slow speech rate (2 syllables per second on average), is it unlikely

959 that resyllabification occurred, so these misclassifications are likely genuine
960 incorrect classifications (i.e. not due to syllabification). As for the normal
961 rate results, there should also exist genuine misidentifications like the slow
962 rate, which is likely why there are onset sequences classified as their coda
963 counterparts. This means that a small number of the NN-resyllabified
964 sequences might be genuine misidentification as well. However, the normal
965 rate results show that onset sequences reached an accuracy rate of 90%
966 and only 36% was achieved for the coda ones. Therefore, a large portion of
967 the NN-resyllabified tokens are likely due to syllabification structure and
968 not just simple false positives.

969 Also, the study did not conduct a parallel analysis of V₂ binary classification
970 for the correctly classified coda tokens. Unlike the DTW analysis, there are
971 too few correctly classified coda sequences in the normal rate for training
972 neural network classifiers, especially for G1 and G2. This issue is
973 exacerbated by the imbalance of speakers in the data, i.e. some speakers
974 had zero or a very small number of correctly classified tokens in certain
975 item groups. Future study can potentially avoid this issue by increasing the
976 number of repetitions in the normal rate condition.

977 Finally, as noted in section IV B, the lack of detectable vowel information in
978 Group 1 might have been avoided had one of the syllables in each pair
979 contained a rounded vowel. This is because, despite its involvement of the
980 tongue-body, the articulation of /s/ is not in direct conflict with the lip

981 movements of the co-produced vowel. This possibility can be investigated in
982 future research.

983 **V. CONCLUSION**

984 We used deep learning models with acoustic data to investigate the
985 phenomenon of resyllabification. The models trained on slow speech data
986 can be used to infer resyllabified sequences in normal speech rate data.
987 This was verified by DTW analysis, which revealed that, compared to slow
988 speech, NN-resyllabified sequences were more similar to the true onset
989 sequences than their original coda productions. The acoustic intervals of
990 intervocalic consonants were examined with bi-directional recurrent neural
991 network models. We found that similar amount of vowel information was
992 detected in the intervocalic consonants between the NN-resyllabified codas
993 and the genuine onsets, suggesting that the coarticulation structure of the
994 former resembles that of the latter. For slow speech rate, the results show
995 that the articulatory structures likely differed between the onset and coda
996 sequences. Surprisingly, however, vowel information can still be detected
997 from the closure and release of labial coda consonants, indicating that the
998 articulation of the vowel has started during the acoustic interval of a coda
999 consonant even when it is not resyllabified.

1000 **APPENDIX**

1001 The hyperparameter details for the multi-class classifier and the binary
1002 classifiers are shown in Table II and Table III, respectively.

1003 TABLE II. Hyperparameters for the multi-class classifiers.

Hyperparameter	Value
Number of residual blocks	3
Number of GRU layers	4
Number of units in the GRU layers	512
Number of units in the linear layers	512
Dropout rate	0.1
Number of channels for the CNN layers	32
Batch size	32
Learning rate	0.0001
Optimiser	RMSprop
Epoch number	120

1004

1005 TABLE III. Hyperparameters for the binary classifiers.

Hyperparameter	Value
Number of units in the first LSTM	60

layer	
Number of units in the second LSTM layer	30
Dropout rate for the first LSTM layer	0.1
Dropout rate for the second LSTM layer	0.2
Number of units in the linear layer	50
Merge mode	Summation
Batch size	16
Optimiser	Adam
Learning rate	0.001
Epoch number	70

1006

1007 ¹During data splitting, correlated samples due to augmentation were not
1008 included in the same dataset. e.g. the original “coo part” and its augmented
1009 version always ended up in the same split.

1010 ²The full detail of models and data processing can be found at
1011 https://github.com/Clara-liu/deep_speech_resyllabification

1012 ³The details of implementation of custom one-inflated-beta-distribution are
1013 available at
1014 [https://github.com/Clara-liu/deep_speech_resyllabification/blob/main/](https://github.com/Clara-liu/deep_speech_resyllabification/blob/main/one_inflated_beta.R)
1015 [one_inflated_beta.R](https://github.com/Clara-liu/deep_speech_resyllabification/blob/main/one_inflated_beta.R)

1016 ⁴See supplementary materials at [URL] for details on the posterior
1017 distributions for the slow rate condition.

1018 ⁵See supplementary materials at [URL] for details on the posterior
1019 distributions for the normal rate condition.

1020 ⁶See supplementary materials at [URL] for details on the posterior
1021 distributions for the duration analysis.

1022 **REFERENCES (BIBLIOGRAPHIC)**

1023 Adda-Decker, M., de Mareüil, P. B., Adda, G., & Lamel, L. (2002).
1024 Investigating syllabic structure and its variation in speech. In
1025 *Pronunciation Modeling and Lexicon Adaptation for Spoken Language*
1026 *Technology* (p. 6).

1027 Amodei, D., Anubhai, R., Battenberg, E., Case, C., Casper, J., Catanzaro, B.,
1028 Chen, J., Chrzanowski, M., Coates, A., Diamos, G., Elsen, E., Engel, J.,
1029 Fan, L., Fougner, C., Han, T., Hannun, A., Jun, B., LeGresley, P., Lin,
1030 L., ... Zhu, Z. (2015). *Deep Speech 2: End-to-End Speech Recognition*
1031 *in English and Mandarin*. <https://doi.org/10.48550/ARXIV.1512.02595>

- 1032 Audacity Team. (2021). *Audacity*. <https://audacityteam.org/>
- 1033 Balakrishnan, N., & Nevzorov, V. (2003). A primer on statistical distribu-
 1034 tions. Hoboken, NJ: John Wiley and Sons.
- 1035 Barlow, J. A., & Gierut, J. A. (1999). Optimality Theory in Phonological
 1036 Acquisition. *Journal of Speech, Language, and Hearing Research*,
 1037 42(6), 1482–1498. <https://doi.org/10.1044/jslhr.4206.1482>
- 1038 Bartelds, M., Richter, C., Liberman, M., & Wieling, M. (2020). A New
 1039 Acoustic-Based Pronunciation Distance Measure. *Frontiers in*
 1040 *Artificial Intelligence*, 3, 39. <https://doi.org/10.3389/frai.2020.00039>
- 1041 Bermúdez-Otero, R. 2011. Cyclicity. In van Oostendorp, M., Ewen, C J.,
 1042 Hume, E., & Rice, K. (Eds.), *Blackwell companion to phonology*.
 1043 Chichester: Wiley-Blackwell, Vol. 4, pp. 2019–2048.
- 1044 Biel, A. L., & Friedrich, E. V. C. (2018). Why You Should Report Bayes
 1045 Factors in Your Transcranial Brain Stimulation Studies. *Frontiers in*
 1046 *Psychology*, 9, 1125. <https://doi.org/10.3389/fpsyg.2018.01125>
- 1047 Birgit A. (2001). Regional Variation and Edges: Glottal Stop Epenthesis and
 1048 Dissimilation in Standard and Southern Varieties of German.
 1049 *Zeitschrift Für Sprachwissenschaft*, 20(1), 3–41.
 1050 <https://doi.org/doi:10.1515/zfsw.2001.20.1.3>

- 1051 Bladon, R. A. W., & Al-Bamerni, A. (1976). Coarticulation resistance in
 1052 English /l/. *Journal of Phonetics*, 4(2), 137-150.
 1053 [https://doi.org/10.1016/S0095-4470\(19\)31234-3](https://doi.org/10.1016/S0095-4470(19)31234-3)
- 1054 Borden, G. J., Harris, K. S., and Raphael, L. J. (2003). *Speech Science*
 1055 *Primer: Physiology, Acoustics, and Perception of Speech, 4th Edition*
 1056 (Williams & Wilkins, Baltimore).
- 1057 Blevins, J. (2003). *Evolutionary phonology: The emergence of sound*
 1058 *patterns*. Cambridge University Press.
- 1059 Boersma, P., & Weenink, D. (2022). *Praat: Doing phonetics by computer*
 1060 (6.2.14) [Computer software]. <http://www.praat.org/>
- 1061 Browman, C. P., & Goldstein, L. (1992). Articulatory Phonology: An
 1062 Overview. *Phonetica*, 49(3-4), 155-180.
 1063 <https://doi.org/10.1159/000261913>
- 1064 Chen, M. Y. (2000). *Tone Sandhi: Patterns across Chinese Dialects*
 1065 (Cambridge University Press, Cambridge, UK).
- 1066 Clements, G. N., & Keyser, S. J. (1983). CV phonology. A generative theory
 1067 of the syllable. *Linguistic Inquiry Monographs Cambridge*, 9, 1-191.
- 1068 Combrisson, E., & Jerbi, K. (2015). Exceeding chance level by chance: The
 1069 caveat of theoretical chance levels in brain signal classification and
 1070 statistical assessment of decoding accuracy. *Journal of Neuroscience*

1071 *Methods*, 250, 126-136.

1072 <https://doi.org/10.1016/j.jneumeth.2015.01.010>

1073 Content, A., Kearns, R. K., and Frauenfelder, U. H. (2001). Boundaries
 1074 versus Onsets in Syllabic Segmentation. *Journal of Memory and*
 1075 *Language* **45**, 177-199.

1076 de Jong, K. J. (2001). Rate-Induced Resyllabification Revisited. *Language*
 1077 *and Speech*, 44(2), 197-216.

1078 <https://doi.org/10.1177/00238309010440020401>

1079 de Jong, K. J., Lim, B., & Nagao, K. (2004). The Perception of Syllable
 1080 Affiliation of Singleton Stops in Repetitive Speech. *Language and*
 1081 *Speech*, 47(3), 241-266.

1082 Dienes, Z. (2014). Using Bayes to get the most out of non-significant results.
 1083 *Frontiers in Psychology*, 5. <https://doi.org/10.3389/fpsyg.2014.00781>

1084 Dienes, Z. (2016). How Bayes factors change scientific practice. *Journal of*
 1085 *Mathematical Psychology*, 72, 78-89.

1086 <https://doi.org/10.1016/j.jmp.2015.10.003>

1087 Douma, JC & Weedon, JT. (2019). Analysing continuous proportions in
 1088 ecology and evolution: A practical introduction to beta and Dirichlet
 1089 regression. *Methods Ecol Evol.* 10, 1412- 1430.

- 1090 Eriksson, A. (2012). Aural/acoustic vs. automatic methods in forensic
1091 phonetic case work. in *Forensic Speaker Recognition* (Springer), pp.
1092 41-69.
- 1093 Gao, H., & Xu, Y. (2010). Ambisyllabicity in English: How real is it? *In*
1094 *Proceeding of the 9th Phonetic Conference of China*, Tianjin.
- 1095 Gao, M. (2009). Gestural coordination among vowel, consonant and tone
1096 gestures in Mandarin Chinese. *Chinese Journal of Phonetics*, 2, 43-50.
- 1097 Garellek, M. (2012). Glottal stops before word-initial vowels in American
1098 English: distribution and acoustic characteristics. *UCLA Working*
1099 *Papers in Phonetics*, 110, 1-23.
- 1100 Garellek, M. (2013). Production and perception of glottal stops (Doctoral
1101 dissertation, UCLA). Retrieved from
1102 <https://escholarship.org/uc/item/7zk830cm>
- 1103 Gaskell, M. G., Spinelli, E., & Meunier, F. (2002). Perception of
1104 resyllabification in French. *Memory & Cognition*, 30(5), 798-810.
1105 <https://doi.org/10.3758/BF03196435>
- 1106 Gelman, A., Carlin, J.B., Stern, H.S., Dunson, D.B., Vehtari, A., & Rubin,
1107 D.B. (2013). *Bayesian Data Analysis* (3rd ed.). Chapman and Hall/CRC.
1108 <https://doi.org/10.1201/b16018>

- 1109 Gick, B. (1999). A gesture-based account of intrusive consonants in English.
 1110 *Phonology*, 16(1), 29–54. <https://doi.org/10.1017/S0952675799003693>
- 1111 Gick, B. (2003). Articulatory correlates of ambisyllabicity in English glides
 1112 and liquids. *Phonetic interpretation: Papers in laboratory phonology*,
 1113 6, 222–236.
- 1114 Goldstein, L., Byrd, D., & Saltzman, E. (2006). The role of vocal tract
 1115 gestural action units in understanding the evolution of phonology. In
 1116 *Action to Language via the Mirror Neuron System* (pp. 215–249).
 1117 <https://doi.org/10.1017/CBO9780511541599.008>
- 1118 Goslin, J., & Frauenfelder, U. H. (2001). A Comparison of Theoretical and
 1119 Human Syllabification. *Language and Speech*, 44 (4), 409–436.
 1120 <https://doi.org/10.1177/00238309010440040101>
- 1121 Gronau, Q.F., Wagenmakers, E.J. Limitations of Bayesian Leave-One-Out
 1122 Cross-Validation for Model Selection. *Comput Brain Behav*, 2, 1–11
 1123 (2019). <https://doi.org/10.1007/s42113-018-0011-7>
- 1124 Harms, C., & Lakens, D. (2018). Making ‘Null Effects’ Informative:
 1125 Statistical Techniques and Inferential Frameworks. *Journal of Clinical*
 1126 *and Translational Research*, 24.
- 1127 He, K., Zhang, X., Ren, S., & Sun, J. (2015). *Deep Residual Learning for*
 1128 *Image Recognition* (arXiv:1512.03385). arXiv.
 1129 <http://arxiv.org/abs/1512.03385>

- 1130 Ioffe, S., & Szegedy, C. (2015). *Batch Normalization: Accelerating Deep*
 1131 *Network Training by Reducing Internal Covariate Shift*
 1132 (arXiv:1502.03167). arXiv. <http://arxiv.org/abs/1502.03167>
- 1133 Iskarous, K., Mooshammer, C., Hoole, P., Recasens, D., Shadle, C. H.,
 1134 Saltzman, E., & Whalen, D. H. (2013). The coarticulation/invariance
 1135 scale: Mutual information as a measure of coarticulation resistance,
 1136 motor synergy, and articulatory invariance. *The Journal of the*
 1137 *Acoustical Society of America*, 134(2), 1271-1282.
 1138 <https://doi.org/10.1121/1.4812855>
- 1139 Jacewicz, E., Fox, R. A., O'Neill, C., & Salmons, J. (2009). Articulation rate
 1140 across dialect, age, and gender. *Language variation and change*,
 1141 21(2), 233-256. <https://doi.org/10.1017/S0954394509990093>
- 1142 Jeffreys, H. (1961). *The theory of probability (3rd ed.)*. Oxford University
 1143 Press.
- 1144 Kahn, D. (1976). Syllable-based generalizations in English phonology.
 1145 ((Doctoral dissertation, MIT).
- 1146 Klatt, D. H. (1976). Linguistic uses of segmental duration in English:
 1147 Acoustic and perceptual evidence. *J. Acoust. Soc. Am.* 59, 1208-1221.
- 1148 Ko, T., Peddinti, V., Povey, D., & Khudanpur, S. (2015). *Audio augmentation*
 1149 *for speech recognition*. Interspeech 2015, 3586-3589.
 1150 <https://doi.org/10.21437/Interspeech.2015-711>

- 1151 Kogan, J. A., & Margoliash, D. (1998). Automated recognition of bird song
 1152 elements from continuous recordings using dynamic time warping and
 1153 hidden Markov models: A comparative study. *The Journal of the*
 1154 *Acoustical Society of America*, 103(4), 2185-2196.
 1155 <https://doi.org/10.1121/1.421364>
- 1156 Lakens, D., McLatchie, N., Isager, P. M., Scheel, A. M., & Dienes, Z. (2020).
 1157 Improving Inferences About Null Effects With Bayes Factors and
 1158 Equivalence Tests. *The Journals of Gerontology: Series B*, 75(1), 45-
 1159 57. <https://doi.org/10.1093/geronb/gby065>
- 1160 Lee, M., & Wagenmakers, E. (2014). Bayesian Cognitive Modeling: A
 1161 Practical Course. Cambridge: Cambridge University Press.
 1162 doi:10.1017/CBO9781139087759
- 1163 Lehiste, I. (1960). An acoustic-phonetic study of internal open juncture.
 1164 *Phonetica Supplement*.
- 1165 Lehiste, I. (1972). The timing of utterances and linguistic boundaries. *J.*
 1166 *Acoust. Soc. Am.* 51, 2018-2024.
- 1167 Lerato, L., & Niesler, T. (2019). Feature trajectory dynamic time warping
 1168 for clustering of speech segments. *EURASIP Journal on Audio,*
 1169 *Speech, and Music Processing*, 2019 (1), 6.
 1170 <https://doi.org/10.1186/s13636-019-0149-9>

- 1171 Levelt, W. J. M., Roelofs, A., & Meyer, A. S. (1999). A theory of lexical
 1172 access in speech production. *Behavioral and Brain Sciences*, 22(01).
 1173 <https://doi.org/10.1017/S0140525X99001776>
- 1174 Liu, Z., & Xu, Y. (2021). *Segmental Alignment of English Syllables with*
 1175 *Singleton and Cluster Onsets*. Interspeech 2021, 3969–3973.
 1176 <https://doi.org/10.21437/Interspeech.2021-187>
- 1177 Liu, Z., Xu, Y., & Hsieh, F. (2022). Coarticulation as synchronised CV co-
 1178 onset – Parallel evidence from articulation and acoustics. *Journal of*
 1179 *Phonetics*, 90, 101116. <https://doi.org/10.1016/j.wocn.2021.101116>
- 1180 Luo, D., Zou, Y., & Huang, D. (2018). *Investigation on Joint Representation*
 1181 *Learning for Robust Feature Extraction in Speech Emotion*
 1182 *Recognition*. Interspeech 2018, 152–156.
 1183 <https://doi.org/10.21437/Interspeech.2018-1832>
- 1184 MacNeilage, P. F. (1998). The frame/content theory of evolution of speech
 1185 production. *Behavioral and Brain Sciences* 21, 499–546.
- 1186 Marin, S., & Pouplier, M. (2014). Articulatory synergies in the temporal
 1187 organization of liquid clusters in Romanian. *Journal of Phonetics*, 42,
 1188 24–36. <https://doi.org/10.1016/j.wocn.2013.11.001>
- 1189 Mirzaei, M. S., Meshgi, K., & Kawahara, T. (2018). Exploiting automatic
 1190 speech recognition errors to enhance partial and synchronized

- 1191 caption for facilitating second language listening. *Computer Speech &*
 1192 *Language*, 49, 17-36. <https://doi.org/10.1016/j.csl.2017.11.001>
- 1193 Mok, P. P. K. (2012). Effects of consonant cluster syllabification on vowel-to-
 1194 vowel coarticulation in English. *Speech Communication*, 54(8), 946-
 1195 956.
- 1196 Morey, R. D., Romeijn, J. W., & Rouder, J. N. (2016). The philosophy of
 1197 Bayes factors and the quantification of statistical evidence. *Journal of*
 1198 *Mathematical Psychology*, 72, 6-18.
- 1199 Mudzingwa, C. (2013). Hiatus resolution strategies in Karanga (Shona).
 1200 *Southern African Linguistics and Applied Language Studies*, 31(1), 1-
 1201 24. <https://doi.org/10.2989/16073614.2013.793953>
- 1202 Mullooly, R. (2003). *An Electromagnetic Articulography study of*
 1203 *resyllabification of rhotic consonants in English*. International
 1204 Conference of Phonetic Sciences, Barcelona.
- 1205 Nakatani, L. H., O'connor, K. D., and Aston, C. H. (1981). Prosodic aspects of
 1206 American English speech rhythm. *Phonetica* 38, 84-106.
- 1207 Nam, H. (2007). *Articulatory modeling of consonant release gesture*.
 1208 International Conference of Phonetic Sciences, Saarbrücken.
- 1209 Nam, H., Goldstein, L., & Saltzman, E. (2009). Self-organization of syllable
 1210 structure: A coupled oscillator model. In F. Pellegrino, E. Marsico, I.

- 1211 Chitoran, & C. Coupé (Eds.), *Approaches to Phonological Complexity*
 1212 (pp. 297-328). Walter de Gruyter.
 1213 <https://doi.org/10.1515/9783110223958.297>
- 1214 Nam, H., Mitra, V., Tiede, M., Hasegawa-Johnson, M., Espy-Wilson, C.,
 1215 Saltzman, E., & Goldstein, L. (2012). A procedure for estimating
 1216 gestural scores from speech acoustics. *The Journal of the Acoustical*
 1217 *Society of America*, 132(6), 3980-3989.
 1218 <https://doi.org/10.1121/1.4763545>
- 1219 Ni Chiosáin, M. N., Welby, P., & Espesser, R. (2012). Is the syllabification of
 1220 Irish a typological exception? An experimental study. *Speech*
 1221 *Communication*, 54(1), 68-91.
 1222 <https://doi.org/10.1016/j.specom.2011.07.002>
- 1223 Ospina, R., Ferrari, S L.P. (2012). A general class of zero-or-one inflated
 1224 beta regression models. *Computational Statistics & Data Analysis*,
 1225 56(6), 1609-1623.
- 1226 Ojala, M., & Garriga, G. C. (2009). Permutation Tests for Studying Classifier
 1227 Performance. *2009 Ninth IEEE International Conference on Data*
 1228 *Mining*, 908-913. <https://doi.org/10.1109/ICDM.2009.108>
- 1229 Park, D. S., Chan, W., Zhang, Y., Chiu, C.-C., Zoph, B., Cubuk, E. D., & Le,
 1230 Q. V. (2019). *SpecAugment: A Simple Data Augmentation Method for*

- 1231 *Automatic Speech Recognition*. Interspeech 2019, 2613–2617.
- 1232 <https://doi.org/10.21437/Interspeech.2019-2680>
- 1233 Pastätter, M., & Pouplier, M. (2014). *The articulatory modeling of German*
- 1234 *coronal consonants using TADA*. International seminar on speech
- 1235 production, Cologne, Germany.
- 1236 Perkell, J., & Chiang, C. M. (1986). *Preliminary support for a ‘hybrid’ model*
- 1237 *of anticipatory coarticulation*. International congress of acoustics,
- 1238 Toronto.
- 1239 Pervaiz, A., Hussain, F., Israr, H., Tahir, M. A., Raja, F. R., Baloch, N. K.,
- 1240 Ishmanov, F., & Zikria, Y. B. (2020). Incorporating Noise Robustness
- 1241 in Speech Command Recognition by Noise Augmentation of Training
- 1242 Data. *Sensors*, 20(8), 2326. <https://doi.org/10.3390/s20082326>
- 1243 Prom-on, S., Xu, Y., & Thipakorn, B. (2009). Modeling tone and intonation in
- 1244 Mandarin and English as a process of target approximation. *The*
- 1245 *Journal of the Acoustical Society of America*, 125(1), 405–424.
- 1246 <https://doi.org/10.1121/1.3037222>
- 1247 Pulgram, E. (1970). *Syllable, word, nexus, cursus* (Mouton, The Hague).
- 1248 Recasens, D. (1984). Vowel-to-vowel coarticulation in Catalan VCV
- 1249 sequences. *J. Acoust. Soc. Am.* 76, 1624–1635.

- 1250 Recasens, D., & Espinosa, A. (2005). Articulatory, positional and
1251 coarticulatory characteristics for clear /l/ and dark /l/: Evidence from
1252 two Catalan dialects. *Journal of the International Phonetic*
1253 *Association*, 35(1), 1-25. <https://doi.org/10.1017/S0025100305001878>
- 1254 Recasens, D., & Espinosa, A. (2009). An articulatory investigation of lingual
1255 coarticulatory resistance and aggressiveness for consonants and
1256 vowels in Catalan. *The Journal of the Acoustical Society of America*,
1257 125(4), 2288-2298. <https://doi.org/10.1121/1.3089222>
- 1258 Redi, L., and Shattuck-Hufnagel, S. (2001). Variation in the realization of
1259 glottalization in normal speakers. *J. Phonetics*, 29, 407-429.
- 1260 Sakoe, H., & Chiba, S. (1978). Dynamic programming algorithm
1261 optimization for spoken word recognition. *IEEE Transactions on*
1262 *Acoustics, Speech, and Signal Processing*, 26(1), 43-49.
1263 <https://doi.org/10.1109/TASSP.1978.1163055>
- 1264 Saltzman, E., & Byrd, D. (2000). Task-dynamics of gestural timing: Phase
1265 windows and multifrequency rhythms. *Human Movement Science*,
1266 19(4), 499-526. [https://doi.org/10.1016/S0167-9457\(00\)00030-0](https://doi.org/10.1016/S0167-9457(00)00030-0)
- 1267 Saltzman, E. L., & Munhall, K. G. (1989). A Dynamical Approach to Gestural
1268 Patterning in Speech Production. *Ecological Psychology*, 1(4), 333-
1269 382. https://doi.org/10.1207/s15326969eco0104_2

- 1270 Schiller, N. O., Mever, A. S., & Levelt, W.J. (1997). The syllabic structure of
1271 spoken words: Evidence from the syllabification of intervocalic
1272 consonants. *Language and Speech*, 40(2), 103-140.
- 1273 Schönbrodt, F. D. & Wagenmakers, E.-J. Bayes factor design analysis:
1274 planning for compelling evidence. *Psychon. Bull. Rev.* 25, 128-142
1275 (2018).
- 1276 Selkirk, E. O. (1982). "The syllable," in *The structure of phonological*
1277 *representations, Part II*, edited by H. v. d. Hulst, and N. Smith (Foris
1278 Publications, Dordrecht, The Netherlands), pp. 337-383.
- 1279 Semeniuta, S., Severyn, A., & Barth, E. (2016). *Recurrent Dropout without*
1280 *Memory Loss* (arXiv:1603.05118). arXiv.
1281 <http://arxiv.org/abs/1603.05118>
- 1282 Sharma, J., Granmo, O.-C., & Goodwin, M. (2020). *Environment Sound*
1283 *Classification Using Multiple Feature Channels and Attention Based*
1284 *Deep Convolutional Neural Network*. Interspeech 2020, 1186-1190.
1285 <https://doi.org/10.21437/Interspeech.2020-1303>
- 1286 Shattuck-Hufnagel, S. (2011). The role of the syllable in speech production
1287 in American English: A fresh consideration of the evidence. In
1288 *Handbook of the Syllable* (pp. 197-224). Brill.
- 1289 Shaw, J. A., Gafos, A. I., Hoole, P., & Zeroual, C. (2011). Dynamic invariance
1290 in the phonetic expression of syllable structure: A case study of

- 1291 Moroccan Arabic consonant clusters. *Phonology*, 28(3), 455–490.
 1292 <https://doi.org/10.1017/S0952675711000224>
- 1293 Smith, J. L. (2001). Lexical Category and Phonological Contrast. *Workshop*
 1294 *on the Lexicon*, 61–72.
- 1295 Soltau, H., Liao, H., & Sak, H. (2016). *Neural Speech Recognizer: Acoustic-*
 1296 *to-Word LSTM Model for Large Vocabulary Speech Recognition*
 1297 (arXiv:1610.09975). arXiv. <http://arxiv.org/abs/1610.09975>
- 1298 Steriade, D. (1999). Alternatives to syllable-based accounts of consonantal
 1299 phonotactics. *Item Order in Language and Speech*, 205–245.
- 1300 Stetson, R. H. (1951). *Motor Phonetics: A study of Speech Movements in*
 1301 *Action*. North Holland.
- 1302 Stone, J. V. (2013). *Bayes' rule: A tutorial introduction to Bayesian analysis*.
 1303 Sebtel press.
- 1304 Strycharczuk, P., & Kohlberger, M. (2016). Resyllabification Reconsidered:
 1305 On the Durational Properties of Word-Final /s/ in Spanish. *Laboratory*
 1306 *Phonology*, 7, 1–24. <https://doi.org/10.5334/labphon.5>
- 1307 Strycharczuk, P., & Scobbie, J. M. (2017). Fronting of Southern British
 1308 English high-back vowels in articulation and acoustics. *The Journal of*
 1309 *the Acoustical Society of America*, 142(1), 322–331.
 1310 <https://doi.org/10.1121/1.4991010>

- 1311 Tiffany, W. R. (1980). "The effects of syllable structure on diadochokinetic
1312 and reading rates," *J. Speech Hear. Res.* **23**, 894-908.
- 1313 Tilsen, S. (2017). Exertive modulation of speech and articulatory phasing.
1314 *Journal of Phonetics*, *64*, 34-50.
1315 <https://doi.org/10.1016/j.wocn.2017.03.001>
- 1316 Tilsen, S. (2019). Motoric Mechanisms for the Emergence of Non-local
1317 Phonological Patterns. *Frontiers in Psychology*, *10*, 2143.
1318 <https://doi.org/10.3389/fpsyg.2019.02143>
- 1319 Tilsen, S. (2020). Detecting anticipatory information in speech with signal
1320 chopping. *Journal of Phonetics*, *82*, 100996.
1321 <https://doi.org/10.1016/j.wocn.2020.100996>
- 1322 Tilsen, S. (2022). *An informal logic of feedback-based temporal control*.
1323 <https://doi.org/10.13140/RG.2.2.14017.28003/1>
- 1324 Tilsen, S., Kim, S. E., & Wang, C. (2021). Localizing category-related
1325 information in speech with multi-scale analyses. *PloS one*, *16*(10),
1326 e0258178. <https://doi.org/10.1371/journal.pone.0258178>
- 1327 Tuller, B., & Kelso, J. A. . S. (1990). Phase transitions in speech production
1328 and their perceptual consequences. In M. Jeannerod (Ed.), *Attention*
1329 *and performance* (Vol. 13). Erlbaum.

- 1330 Tuller, B., & Kelso, J. A. . S. (1991). The production and perception of
1331 syllable structure. *Journal of Speech and Hearing Research*, 34, 501–
1332 508.
- 1333 Uffmann, C. (2007). Intrusive [r] and optimal epenthetic consonants.
1334 *Language Sciences*, 29(2-3), 451–476.
- 1335 Wagenmakers, E.-J., Morey, R. D., & Lee, M. D. (2016). Bayesian benefits
1336 for the pragmatic researcher. *Current Directions in Psychological*
1337 *Science*, 25(3), 169–176.
- 1338 Wagner, M. (2005). Prosody and Recursion. (Massachusetts Institute of
1339 Technology).
- 1340 Wang, C., Xu, Y., and Zhang, J. (2019). Mandarin and English use different
1341 temporal means to mark major prosodic boundaries. in *The 19th*
1342 *International Congress of Phonetic Sciences* (Melbourne, Australia).
- 1343 Wu, S.-L., Shire, M. L., Greenberg, S., & Morgan, N. (1997). Integrating
1344 syllable boundary information into speech recognition. *1997 IEEE*
1345 *International Conference on Acoustics, Speech, and Signal*
1346 *Processing*, 2, 987–990. <https://doi.org/10.1109/ICASSP.1997.596105>
- 1347 Xu, A., Birkholz, P., & Xu, Y. (2019). *Coarticulation as synchronized*
1348 *dimension-specific sequential target approximation: An articulatory*
1349 *synthesis simulation*. 205–109.

- 1350 Xu, Y. (1986). Acoustic-phonetic characteristics of junctures in Mandarin
1351 Chinese. *Journal of Chinese Linguistics*, 4, 353-360.
- 1352 Xu, Y. (2020). *Syllable is a synchronization mechanism that makes human*
1353 *speech possible* [Preprint]. PsyArXiv.
1354 <https://doi.org/10.31234/osf.io/9v4hr>
- 1355 Xu, Y., & Liu, F. (2006). Tonal alignment, syllable structure and
1356 coarticulation: Toward an integrated model. *Italian Journal of*
1357 *Linguistics*, 18, 125-159.
- 1358 Xu, Y., & Liu, F. (2007). Determining the temporal interval of segments with
1359 the help of F0 contours. *Journal of Phonetics*, 35(3), 398-420.
1360 <https://doi.org/10.1016/j.wocn.2006.06.002>
- 1361 Zhang, X., Sun, J., & Luo, Z. (2014). One-against-All Weighted Dynamic
1362 Time Warping for Language-Independent and Speaker-Dependent
1363 Speech Recognition in Adverse Conditions. *PLoS ONE*, 9(2), e85458.
1364 <https://doi.org/10.1371/journal.pone.0085458>